DESIGNING AND IMPLEMENTATION OF INTERFACING CIRCUIT FOR CM OF HV UG CABLES

A Dissertation submitted in partial fulfillment of the requirements for the award of degree

Of

MASTER OF ENGINEERING

In

Power Systems

Submitted by

Gurdamandeep Singh

(Regn. No. 801341004)

Under the guidance of

Mr. Shailesh Kumar

Lecturer, EIED

JULY 2015

Electrical and Instrumentation Engineering Department

Thapar University, Patiala

(Declared as Deemed-to-be-University u/s 3 of the UGC Act., 1956)

Post Bag No. 32, Patiala – 147004

Punjab (India)

CERTIFICATE

I hereby certify that the work which is being presented in the dissertation entitled, **"Designing and Implementation of an Interfacing Circuit for Condition Monitoring of HV Underground Cables "**, in partial fulfillment of the requirements for the award of degree of Master of Engineering in **Power Systems** submitted in Electrical and Instrumentation Engineering Department of Thapar University, Patiala, is an authentic record of my own work carried out under the supervision of Mr. Shailesh Kumar, Lecturer, EIED.

The matter presented in this thesis has not been submitted for the award of any other degree or diploma anywhere.

Gurdamandeep Singh

(Gurdamandeep Singh)

This is to certify that the above statement made by the candidate is true to the best of my knowledge and belief.

Shailesh Kr. 13/7/2015

(Mr. Shailesh Kumar)

Lecturer

Electrical & Instrumentation Engineering Department

Thapar University

Patiala

Countersigned by

(Dr. Ravinder Agarwal)

Professor & Head

Electrical & Instrumentation Engineering Department

Thapar University, Patiala

(Dr. S.S. Bhatia)

Dean (Academic Affairs)

Thapar University

Patiala

ACKNOWLEDGEMENT

I would like to express my sincere gratitude to my supervisor, **Mr. Shailesh Kumar**, Lecturer, Electrical and Instrumentation Engineering Department, Thapar University, Patiala for his guidance, meticulous efforts, constructive criticism, inspiring encouragement, unflinching support and invaluable co-operation which enabled me to enrich my knowledge and reproduce it in the present form.

I also like to extend my gratefulness to **Dr. Ravinder Agarwal**, Professor and Head, Electrical and Instrumentation Engineering Department, Thapar University, Patiala for his perpetual encouragement, generous help and inspiring guidance.

I am very grateful to **Ms. Manbir Kaur**, Associate Professor and PG Coordinator, Electrical and Instrumentation Engineering Department, Thapar University, Patiala for her co-ordination throughout my M.E. Degree.

I am also very thankful to the entire faculty and staff members of Electrical and Instrumentation Engineering Department for their direct–indirect help, co-operation, love and affection, which made my stay at Thapar University memorable.

I wish to thank all my classmates for their time to time suggestions and cooperation without which I would not have been able to complete my work.

Gurdamandeep Singh

(801341004)

ABSTRACT

It is well known fact that the moisture content and heat generated from the cables deteriorates the insulation resistance and the cable sheath. For the comfort and reliable transaction of power of buried cables, high voltage cables are used. Oil-filled high voltage cable is most commonly used for well transmission and distribution of electrical energy. Oil-filled (132-500 kV) are laid in specially constructed concrete lined trenches. Surroundings of the cores are the combination of filler material giving the mechanical support with the capacity to conduct heat away from the cables. The ampacity of the cable to function within its characteristics and overall the structure life-time is influenced by the thermal conductivity of the adjacent materials. With the increase in moisture content, thermal conductivity also increases.

For computing the data analysis of moisture content and temperature inside the cable conduit, I have designed an interfacing circuit for condition monitoring of HV buried cables which works on a relaxation oscillator phenomena and based on a Wheatstone bridge. The designed interfacing circuit utilizes two different resistive sensors (impedance moisture sensor and temperature sensor) for converting incremental resistance change due to the moisture and the temperature due to the thermal stress into frequency and duty cycle respectively. The change in resistance to the original resistance of the sensor is proportional to the moisture ingress onto the moisture sensor available in the filler material of the UG cable. This circuit is simulated on a NI Multisim software and hardware implemented on a breadboard. Both simulation results and experimental results have been captured obtained from oscilloscope is presented.

TABLE OF CONTENTS

LIST OF FIGURES

\

LIST OF ABBREVIATIONS

OP-AMP	Operational Amplifier
PWM	Pulse Width Modulated
DTS	Distributed Temperature Sensor
PD	Partial Discharge
PCB	Printed Circuit Board
UG	Underground Cable
RTD	Resistance Temperature Detector
PVC	Poly Vinyl Chloride
VIR	Vulcanised India Rubber
XLPE	Cross Linked Polythene
AC	Alternating Current
DC	Direct Current
RMS	Root Mean Square
DC	Duty Cycle
VCO	Voltage Controlled Oscillator
ADC	Analog-to-Digital Converter
RC	Resistor Capacitor
IC	Integrated Circuit
CRO	Cathode Ray Oscilloscope

CHAPTER1

INTRODUCTION

1.1 OVERVIEW

The concept of overhead lines was engaged in underground work in the very early days of transmission of power. Basically, a combination of the conductor and its insulation is called a cable. In massively populated areas of towns and cities, the transmission and distribution of electrical energy is done by underground cables for the safer and reliable point of view. The permissible loading of the cables is governed by various parameters such as environmental conditions, operating conditions, insulation type, type of laying, cable design and so on. External protection on the cable against moisture entry, chemical reaction and mechanical injury etc. is provided. Thermal resistivity of soil is one of the most important factors affecting the underground cable ampacity. Ampacity is defined as the current that a conductor can carry constantly within a precise environment including power loss, temperature rating and heat dissipation etc. and this current is in amperes [1].

In the present time when underground transaction of power is required at high voltage levels, high-voltage cables are used. Oil filled cable is one of the most useful type of high-voltage underground cables. Oil filled high voltage cable (132-500 Kv) is laid in especially constructed culverts or ducts or may be concrete tunnels.

Immediate core of the oil filled cable is the single or the combination of one or more filler materials offering great mechanical strength with the potential to conduct heat away from the cables. The capacity of the cable is to function within its properties and overall the structure life time is influenced by the thermal conductivity of the nearby materials. Thermal conductivity is determined by the quantity of moisture content in the filler material, such that an increase in moisture content will give an increase in thermal conductivity and vice-versa. Calculating the maximum loading of the circuit during this period, distinct value of thermal conductivity is used for the wet material in winter months and accurate value is used for the dry material in summer months.

A condition can occur where the rise in the temperature of the cable causes the total rise in resistance in enormously conditions of dry out. This type of situation can rapidly assist to fatal thermal runaway without observed closely [2]-[3].

The estimate of temperature of the underground cables can be governed by taking with a resistive thermometer and the temperature of a conduit adjacent to the cable which is the source of heat. The resistive sensors are employed for the sensing purpose and considered to measure the soil resistance and temperature resistance in terms of voltage signals. A relevant voltage signal is required which would change as the change in level of moisture of the surrounding soil [4].

In this project work, I have designed a linear and sensitive Wheatstone bridge based interfacing circuit for a pair of resistive sensors which works on a relaxation oscillator phenomenon for converting incremental resistance change due to the moisture in the sand adjacent to the cable and change in temperature due to the high thermal stress on the cable in terms of frequency and duty-cycle simultaneously for condition monitoring of high voltage underground cables. This interfacing circuit is simulated on National Instruments (NI) Multisim 13.0 software. These two types of resistive sensors which transforms one form of physical quantity into another form and also perform an input function because they can sense a moisture or temperature quantity and translate it into an electrical signals i.e. are frequency and duty-cycle. Hence the current design offers both the aspects i.e. frequency and duty cycle carry information at the same time from two different resistive sensors (impedance moisture sensor and temperature sensor).

The frequency of the PWM output signal is varied by the primary (impedance moisture) sensor and the duty cycle is individually controlled by the secondary (thermal) sensor. The change in resistance to the original resistance ($\Delta R/R$) is proportional to the moisture ingress onto the moisture sensor available in the filler material and change in resistance due to change in temperature inside the core of the cable is turned into the frequency and the duty cycle. Further, the duty cycle is simply converted into DC analog signal by applying the pulse width modulated (PWM) wave to a low pass RC filter [5].

1.2 DISSERTATION LITERATURE SURVEY

Here is the survey of some literature that is significant to convey out this thesis work.

Anders G. A. *et. al* has presented the new formula to measure the ampacity and internal thermal resistance of the 3-core cables. He supposed that the insulation and the available filler material of 3-core underground cable have the similar thermal resistivities. He has also described the effect of the thermal resistivity on ampacity of the cable by using the different parameters of the cable **[1]**.

Martin G. Stewart *et. al* described a moisture sensor which is used to evaluate the moisture content available in the filler material of the trough of underground cable. He has designed an interfacing circuit between sensor probe and SCADA (Supervisory control and acquisition data) system for online condition monitoring in the troughs of high-voltage cables. The calculation of maximum circuit loading at different climatic conditions has been also discussed **[2]**.

Malmedal K. *et. al* has defined the soil thermal resistivity is directly proportional to the moisture content. He has presented that the heat produced by the underground power cables is the major reason to affecting the thermal resistivity of the soil. The process of heat transfer from the power cables has also been illustrated **[3]**.

Imlay L. E. *et. al* explained the effects of moisture content in the soil on the temperature of underground cables. He has discussed the different methods that are used for decreasing the temperature and increasing the current carrying ability of the cable. He has also suggested that the estimated temperature of underground cables is found with the help of resistive thermometer **[4]**.

Tarikul Islam *et. al* illustrated the simply signal conditioning circuit for a particular purpose for a resistive humidity sensor and temperature detector sensor. It is a relaxation oscillator technique based an improved form of Wheatstone bridge for the linearly conversion of resistance into frequency and duty-cycle respectively. He has discussed for controlling the temperature error of the resistive moisture sensor. The fabrication, characteristics and its working of a sol-gel thin film structure based resistive humidity sensor has been discussed by him. The author deliberated the frequency relation for an active bridge circuit for strain gauge applications **[5]**.

Taranovich S. *et. al* has stated the basic terms used in humidity sensors. The various kinds of resistive sensors have been presented like relative humidity sensors, absolute humidity sensors and capacitive humidity sensors. The signal conditioning circuit based on a resistive humidity sensors has been designed also **[6]**.

Farhani Hamid *et. al* has presented the fabrication technologies, sensing substrates and working principle of the resistive humidity sensors. The uses of resistive type humidity sensors also have been discussed **[7]**.

M. L. Soni *et. al* introduced the classification of cables and insulation used in it. He has described the constructional features of oil-filled and gas-filled high voltage underground cables and its uses **[8]**.

Eby E. D. *et. al* described the representative designing and dielectric testing of oil-filled HV underground cables. The factors determining the transmission of carrier current have been presented **[9]**.

Arman A. N. *et. al* presented the power rating of the high-voltage cable which is affected by the migration of moisture in the soil. He has assumed the method for the calculation of current rating on the account effect of migration of moisture from the sand around a cable. The modified rating parameters for prevention from moisture migration are derived by using this method **[10]**.

Starr A. T. *et. al* has introduced the manufacture of different types of underground power cables and its laying. He has also explained the breakdown and thermal characteristics of buried cables **[11]**.

Bascom E. C. *et. al* introduced with basic components of the cable and its system types i.e. are extruded dielectric type cable, pipe type cable and self-contained fluid filled type cable. He has presented the ampacity and soil thermal testing of the different kinds of underground cables. He has been also described the temperature monitoring systems by using distributed temperature sensors (DTS) and different installation methods of underground cables **[12]**.

Schurig O. R. *et. al* illustrated the various types of losses occurred in the armoured single core conductor underground cables i.e. are dielectric losses, conductor losses and lead sheathed circulating current losses **[13]**.

Cramp W. *et. al* illustrated the Arnolds formula to calculate the sheath losses due to eddy currents. He has also calculated the eddy currents of 3-core underground cable **[14]**.

Shaklin G. B. *et. al* devised the influences of moisture on the thermal conductivity of the soil around the underground cables. He has explained the Intersheath losses generated in the power cables due to rise in temperature **[15]**.

Wadhwa C. L. *et. al* described the sheath eddy current and sheath circuit current losses produced in the underground power cables due to the heat produced in it **[16]**.

Lucas J. R. *et. al* introduced the concept of cross bonding using linear and non-linear resistor earthing during fault conditions **[17]**.

Naskar A. K. *et. al* presented the two dimensional finite element method for temperature analysis of underground cables. This method is used to evaluate the steady-state temperatures at several points of the cable system. He has been applied this method to 3-core, 6600 volts underground cable and calculate the steady-state copper losses originates in the cable **[18]**.

El-Kady M. A. *et. al* has introduced the technique for calculating the temperature rise and load capabilities of power cables with provision for statistical variations of various soil, boundary and loading conditions **[19]**.

Neher J. H. *et. al* has solved the problem regarding the temperature rise of buried cables and its pipes. He has developed the formulae for computing this temperature rise as a function of heat loss and their thermal resistivities. He has also explained the moisture migration and thermal resistivity of the soil **[20]**.

Brooks E. J. *et. al* devised the controlling technique of moisture content in the environment of the cable with the help of cable culverts. The heat dissipation rate generated from underground cables is mainly depending upon the thermal resistivity because of soil drying. The different types of methods for heath test installation of the power cables have been presented **[21]**.

Vittorio Ferrari *et. al* designed the signal conditioning circuit for two different resistive sensors based on a relaxation oscillator phenomena in which the pulse width modulated (PWM) wave output signal carry information at the same instant in the form of both frequency and duty-cycle.

He has adopted the method for compensating the accuracy deterioration initiated by the finite switching delays and output results on its experimental analysis are described **[22]**.

Huijsing H. J. *et. al* designed the signal conditioner circuit for voltage to current converter for computing the output voltage of the open Wheatstone bridge. These types of circuits are used for remote transmission of analog signals **[23]**.

Mochizuki K. *et. al* designed the basic configuration of temperature to frequency converter comprises of a Wheatstone bridge which is followed by an integrator and a comparator and works on a integrable colpitts oscillator whose frequency varies linearly with a change in resistance identified by the bridge balancing factor. He suggested that this resistance to frequency converter is best suitable for an interfacing with resistive sensors. **[24]**.

Mantenuto P. *et. al* purposed the analog interfacing circuit based on a uncalibrated bridge for the continuous approximation of the output voltage signal. They will be implemented the interfacing circuit on a PCB and experimental results have been captured **[25]**.

Johnson C. D. *et. al* designed the circuit for linearly converting resistance into frequency with the switching device as a MOSFET instead of a diode. He has also used the zero crossing detector and multivibrators configuration **[26]**.

Gouda O. E. *et.al* investigated the influence of the formation of the dry zone on the cable ratings of the high-voltage underground power cables. The capacity, de-rating factor and the temperature compensation of underground cables also have been discussed **[27]**.

Khan A. A. *et. al* described the different types of diagnosis and condition monitoring techniques which provides the necessary information for the safer, reliable, electrical aging and replacement plan for the insulation of underground power cables such as partial discharge (PD) monitoring, current leakage monitoring and temperature monitoring. He has mainly focused on partial discharge monitoring which are of two types; online partial discharge (PD) monitoring and offline partial discharge monitoring. The information received by online PD monitoring can helps in detecting the upcoming faults and estimates the remaining life of the cable insulation **[28]**.

Lyal J. S. *et. al* demonstrated the automated online condition monitoring system and its analysis for underground cables for measuring the thermal resistivity and the thermal conductivity**[29]**.

Lee C. Y. *et.al* presented the high frequency partial discharge (PD) measurement technique for the monitoring of cable system by using capacitive sensors instead of using resistive sensors. This capacitive sensor is fixed inside the cable junctions and ends without affecting the design of the cable insulation. He has shown that resistance occurred between the sensor and the ground sheath affecting the sensitivity of the sensor **[30]**.

1.3 OBJECTIVE OF THE THESIS

The objective of the present work is to design and implemented a resistance to frequency and duty-cycle conversion scheme which linearizes the output frequency related to the resistive unbalance factor of a Wheatstone bridge, while the duty-cycle is independently controlled by the thermal sensor. This scheme provides an accurate data for monitoring of underground cables in electrical power system in terms of frequency and duty-cycle.

1.4 ORGANISATION OF THE THESIS

The thesis work has been summarized in five chapters:-

In chapter 1 briefs the overview of the present work, literature survey and objective of the thesis, problem statement and scope of the thesis.

In chapter 2 introduces the resistive sensors and its types.

In chapter 3 discusses the underground cables and its insulation classification. The various types of losses generated in the UG cables.

In chapter 4 deliberates the resistance to frequency and duty-cycle conversion scheme and briefly explanation of each components used in this scheme.

In chapter 5 simulation of an interfacing circuit and its results. Experimental setup and its output results also have shown in this chapter.

In chapter 6 this chapter contains conclusion and future scope of the thesis work.

CHAPTER 2

RESISTIVE SENSORS

2.1 INTRODUCTION

Moisture content measurement is one of the most extensive process parameters in the field of automated systems, instrumentation and its control. Generally, moisture sensors are of either the resistive type or the capacitive type. Mostly moisture sensors are impedance technology dependent. These types of sensors are fabricated from either the ceramic or the polymer material. Resistive type sensors are used to about 20 to 90 percent of relative moisture. It generally comprises of a hygroscopic medium which absorbs moisture content from material dropped onto the metal electrodes on a substrate of non-conductive type. These resistive sensors enumerate the change of moisture and translate it into the change in electrical conductance (impedance) of the hygroscopic medium. When the resistive moisture sensor is placed in the material with the existence of water vapour, it absorbs moisture causing the ions to isolate and results in higher conductivity.

2.2 RESISTIVE IMPEDANCE MOISTURE SENSOR

The impedance moisture sensors are most widely used in industries to maintain the working temperature for the purpose of machine efficient. The moisture sensor is rugged in construction and can work at very high temperatures. Due to its accuracy, high reliability, high repeatability and response at fast speed, these moisture sensors are used to measure the humidity in atmospheric air and gases. The main use of impedance moisture sensor is where the wide dew point range is required. The accuracy of measurement of this type of sensor is about up to ± 1℃ dew point [6].

2.3 RESISTANCE TEMPERATURE DETECTOR (RTD)

It is a temperature sensor having variable resistive value as the temperature changes. These are mostly used in automated industries due to its high repeatability and stability. The stability of these sensors is improved by using platinum and prevents them from corrosion or oxidation. RTDs are used instead of thermocouples due to their better accuracy. Therefore the level of the

moisture increases with the decrease in the resistance of the sensor. Therefore, the variation in resistance is more important and can be simply interfaced by the current interfacing circuit.

The sensitivity of the sensor is governed using following expression:-

$$\left(\frac{\Delta R}{R}\right) \div \left(\frac{\Delta R_m}{R_m}\right) \times 100 \tag{2.1}$$

The variation in the resistance of the sensor due to working temperature depends on the material by which the sensor is made [7].

Two dissimilar kinds of resistive sensors are employed in this interfacing circuit i.e. are resistive moisture sensor and temperature detector sensor (TDS) which carries the simultaneously information of moisture content due to the change in resistance of the sensor and change in temperature due to the thermal stress on the cable in the form of frequency and its duty cycle. The impedance moisture sensor is placed in the Wheatstone bridge for the variation in frequency while the temperature detector sensor is across the inverting mode operational amplifier for the variation in duty-cycle.

CHAPTER 3

UNDERGROUND CABLE

3.1 INTRODUCTION

Through continuous research and development in the field of high-voltage underground cables, the brilliant functions of oil filled high voltage underground cable have been improved since 1900 century. Some brilliant characteristics of the oil filled cables are as under

1) Large operating potential gradient therefore the thickness of the insulation is selected as thin.
2) No void in the cable insulation and electrically stable.
3) Contraction and expansion of insulating oil due to temperature change can be easily compensated by the oil reservoirs.
4) Self-monitoring of the cable.

Due to the lower spacing between the conductor and earth, high-voltage underground cables have a much lower inductance than overhead lines but correspondingly higher capacitance and thus a much higher charging current. There is a hazard of breakdown of the dielectric on the statement of existence of voids in the extra high-voltage cables. Failure of the dielectric constant results in ionization and associated chemical reactions which harm the insulation of the cable. To minimize the formation of voids the two methods are generally used

1) Using thin oil under some pressure (Oil filled cables).
2) Using nitrogen gas pressure at 12-15 atmospheres (Gas filled cables).

3.2 OIL-FILLED CABLE

Oil filled cable comprises of a concentric type stranded conductor built around an open helical core that works as a channel for the flow of oil. In this type of cable, oil is regularly supplied from the oil reservoirs which are placed near the cable sheath. The ducts within the core of the cable are attached to these oil reservoirs and thus compression or expansion of the oil in the oil filled cable does not create any gap. The conductor in these cables, must be completely insulated hence air does not form portion of the insulation.

Single phase $(1-\phi)$ oil filled cables are most commonly used in high-voltage systems However 3-core oil filled underground cables exist. Generally, high-voltage cables are single cored and thus have their separate mechanical protection and insulation by sheaths.

Normally 1-core cables are employed as three core cables are too much large and difficult to move because of its shape, size and weight but there are more sheath losses in 1-core cable and thus they are not usually armoured. The 3-core cable has the cores formed together and each core being insulated. Further three cores are insulated with impregnated paper and at last lead sheath shield the all 3-cores to avoid moisture entering to the cable. The below figure shows the constructional structure of single core oil-filled cable in figure 3.1:

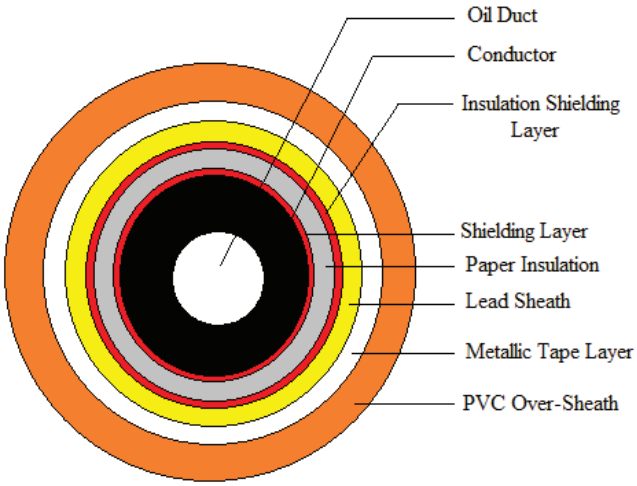

Figure 3.1 Constructional view of oil-filled cable

The 3-core oil filled cables may be of flat type or may be conventional circular design. The flat sides of cable are strengthened with binding wires and metallic tapes. Pumps are used to maintain specified pressure of the oil and it should not fall below 22 kN/m^2. The voltage stress up to 130 kV/cm can sustain by oil filled high-voltage underground cables [8]-[10].

The existence of the lead sheath creates certain difficulties as currents are induced in the sheath as well. It is due to the fact that sheaths of conductors cuts the magnetic field introduce by the conductors. The magnetic field is not the same at all the points along the cable routes. Therefore different voltages are induced at different points on the sheath.

This causes to flow eddy currents in the sheath. These eddy currents mostly depend upon the following factors which are as follows.

a) Distance between the cables.
b) Resistivity (ρ) of the sheath material.
c) Operating frequency.
d) Mean radius of the sheath.

3.3INSULATIONS USED IN UG CABLES

Insulation is used in the cable to cover the conductor so as to isolate it from the surroundings. The insulation should have high dielectric strength, good mechanical potency, high resistance and high thermal resist capability. The insulation of the cables which are generally used as under.

3.3.1 POLY VINYL CHLORIDE (PVC)

Poly vinyl chloride is a synthetic material and is governed as white odourless, non-inflammable, chemically inert to oxygen and almost inert to many acids and alkalies, tasteless and insoluble powder. It is a material having good dielectric strength, high melting temperatures and high insulation resistance. It is chemically linked with a plastic compound and the gel is used as in the form of insulation cover over the conductor of the core. It has dielectric strength of 17 kV/mm, dielectric constant of 5 and continuous maximum temperature rating of 75^{o} C.

3.3.2 VULCANISED INDIA RUBBER (VIR)

During1880-1930, this cable insulation was developed in the early steps of cable manufacture. However it has got reasonably good dielectric strength of 15 kV per mm but its use is limited due to its low melting point, less chemical resistance capability and short period of life. These types of cables are light weighted in respect with paper insulated and lead covered cables. In the present days, they are not now manufacture because of softening and decentralization and are being swapped by the paper insulated cables due to cheaper and greater current carrying capability [11].

3.3.3 PAPER INSULATION

Paper insulation is one of the most important insulation still now for manufacturing of high-voltage power cables and is made up of manilla hemp from fibre and wood pulp. It is highly preferable as insulating medium because of its higher dielectric strength, thermal conductivity; high durability and better temperature withstands ability. The dielectric constant is 3.5 whereas dielectric strength is around 20 kV per mm and can be employed for continuous maximum temperature rating of 80-85^{o} C.

3.3.4 CROSS LINKED POLYTHENE (XLPE)

The cross linking of carbon atoms and compound with low density polythene is a new insulating material having low dielectric constant, high mechanical strength, small dimension with light weight and high melting point.

This type of cable has dielectric strength of 20 kV/mm with high continuous maximum temperature rating of 90^{o} C. XLPE cables permit the temperature of conductor of 90^{o}C and 250^{o}C under normal and short circuit conditions.

Cross linked poly ethane material has temperature range from 250^{o}C to 300^{o}C and gives better insulating properties. Cross linked polythene (XLPE) cables can be buried directly on the soil bed and easily suitable for the voltages up to 33 kV because of its low moisture absorption and high temperature withstand capability [12].

3.4 TRANSFER OF HEAT IN CABLES

The power losses in the cable conductor, cable insulation, cable sheath and other constituents of cable which act as a heat source. It causes the temperatures of many cable components to rise above the ambient temperature. There are a variety of reasons that can occur power loss in the cable and are shown in below figure. They may be caused due to the conductor current passing through the resistance of the conductor of core of the cable and is called conductor loss and also sometimes called the copper loss because conductors were generally made out of copper (Cu).

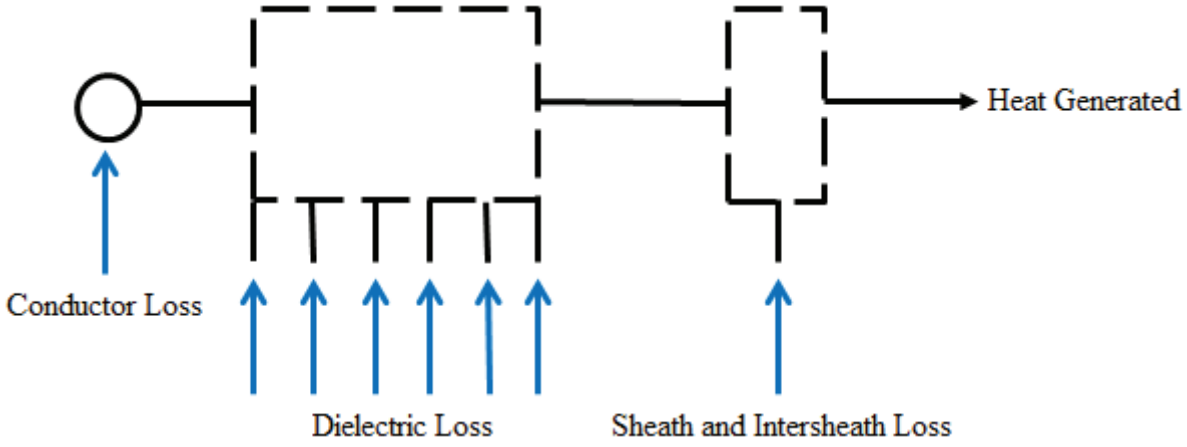

Figure 3.2 Heat transfer in the cable

The power loss caused by the over and under voltage across the insulation and sheath losses are occurred due to the induced currents in the sheath. The circulating currents in the loops formed between the sheaths of different phase's results in intersheath losses. The conductor losses, sheath losses and intersheath losses are current dependent while dielectric loss is depend on the current.

3.4.1 CONDUCTOR LOSS

The conductor loss (P_{con}) is stated by the following expression

$$P_{con} = I^2 \times R_{con} \text{ Watt} \tag{3.1}$$

Where 'I' is the current in the cable and 'R_{con}' is the resistance of the conductor.

3.4.2 DIELECTRICLOSS

The power factor is zero for an ideal dielectric. Subsequently the power factor is not zero for a non-ideal dielectric. Therefore, the current leads voltage by an angle less than 90^o and thus there is a power loss in the cable. Dielectric loss is the loss in the cable because of leakage resistance. If C_c is the capacitance of the cable and E_{av} is the voltage to be applied or phase voltage then charging current (i_c) and power loss (P_L) is given as follows

$$\text{Charging current } (i_c) = E_{av}\ C_c\ \omega \tag{3.2}$$

Hence the power loss (P_L) in the cable is given as under expression:

$$P_L = E_{av}\ I\ cos\theta \tag{3.3}$$

$$= E_{av}\ I\ cos\,(90° - \psi\,)$$

$$= E_{av}\ I\ sin\psi$$

$$= E_{av}(i_c / cos\psi) \times sin\psi$$

$$P_L = E_{av}^2\ C_c\ \omega\ tan\psi \text{ .....W/phase} \tag{3.4}$$

Where angle 'θ' is the power factor angle of dielectric'ψ' is the dielectric loss angle in radians [13].

3.4.3 SHEATH LOSS

The alternating currents (A.C.) flowing through the cable create pulsating magnetic field in the single core cables when used for A.C. transmission. This pulsating electro-magnetic field links with the lead sheath of the cable and produces voltage in it. This produced voltage originates currents under some special conditions in the sheaths and this consequence in sheath losses. Since the sheath loss is proportional to the conductor loss. The equivalent resistance (A.C.) of the cable is determined by the following expression:

$$R_{eq} = R_c\,(1+\alpha) \tag{3.5}$$

Where 'R_c' is the resistance of the cable core and 'α' is the ratio of sheath loss to the conductor loss. Two kinds of sheath currents in the sheath losses are briefly discussed below

1) Sheath eddy currents.
2) Sheath circuit currents.

1) **Sheath eddy currents: -**These type of currents flow merely in the sheath of the same cable. This type of currents will flow through the sheath of the cable when the two cable sheaths are unconnected at both the ends or when they are linked at one end only.

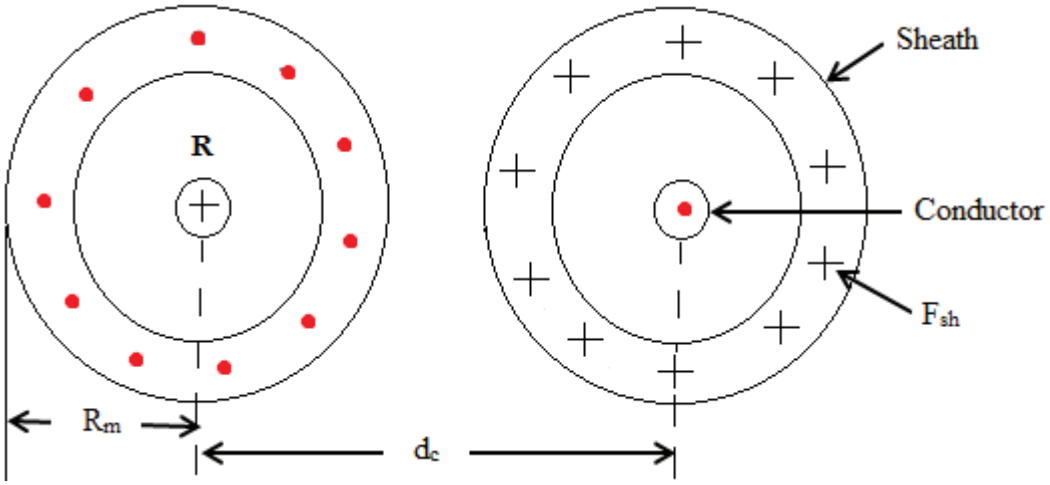

Figure 3.3 Sheath losses in single phase underground cable

The voltage which originates in a two cable system in the sheath of an individual cable. Now the voltage produced in the sheath of a cable due to current in the cable core is given as follows.

$$E_s = \omega \times I \times M_s \tag{3.6}$$

Where 'E_s'the voltage is induced in the sheath of a cable, 'I' is the current in the core of the cable and 'M_s' is the mutual inductance between the cable core and the sheath of an adjacent cable. Mutual inductance (M_s) between the sheath and the core of the cable by definition states the flux linkages that link both the sheath and the core due to the current (I) in the cable core, the current per ampere carried by the core of the cable.

$$M_s = 2\times10^{-7} ln\left(\frac{d_c}{R_m}\right) \text{Henry/metre} \tag{3.7}$$

Therefore, $E_s = \omega \times I \times M_s$

$$= I \times \omega \left[2\times10^{-7} ln\left(\frac{d_c}{R_m}\right)\right]$$

$$E_s = \left[2 \times I \times \omega \times ln\left(\frac{d_c}{R_m}\right)\right] \times 10^{-7} \text{ Volts/metre} \tag{3.8}$$

If the sheaths of the cable are bounded at one end only, then the voltage between the two sheaths at the far end will be given as under.

$$2E_s = 2 \times \omega \times I \times M_s \tag{3.9}$$

$$2E_s = \left[4 \times 10^{-7} \times I \times \omega \times ln\left(\frac{d_c}{R_m} \right) \right] \text{Volts/metre} \tag{3.10}$$

Under the circumstances of the short circuit, the currents are of larger magnitudes which bring in high voltages between the sheaths and in this case sheaths are not bonded.

The sheath losses occurring in the cable are usually governed by the empirical formula for sheath losses because of sheath eddy currents is suggested by Arnold. Arnold's approximate formula for the sheath loss due to sheath eddy current is described as

$$\text{Sheath eddy current loss } (P_s) = I^2 \left[\frac{3\omega^2}{R_s} \left(\frac{R_m}{d_c} \right)^2 \times 10^{-18} \right] \text{Watts/cm/phase} \tag{3.11}$$

Where 'I' is the current per conductor in Amperes in cable.

'R_s' $\rightarrow$ Sheath resistance in ohms.

'R_m' $\rightarrow$ Mean radius of the sheath.

'd_c' $\rightarrow$Distance between the conductors from centre-to-centre.

The sheath losses are usually very small and are generally about 2-5% of the conductor loss and thus normally neglected. Hence dielectric loss, conductor loss and sheath loss combine constitute to the heating of cables.

2) **Sheath circuit currents: -**while the rest type of currents flow from sheath of one cable to another cable sheath and is known as bonding of the cables thus sheath circuit currents are absent in unbounded type of cables. Due to the high voltages produced between the sheaths when they are unbounded under short circuit conditions, it is normally considered fine practice to bond the sheaths at both ends [14]-[16].

3.4.4 INTERSHEATH LOSS

This loss is caused by the induced voltage between the sheaths and causing a circulating current in the cable. When the sheaths of the adjacent cables are connected together then this loss is only present. The Sheaths need to be connected jointly in normal practically, as otherwise sparking in the core of the conductor and causing harm to the cable sheaths. The mutual inductance (M_s) between the core of single cable and an adjacent cable sheath is given below

$$M_s = 2\times10^{-7} ln\left(\frac{d_c}{R_m}\right) \text{Henry/metre} \tag{3.12}$$

The voltage produced (E_{is}) in the Intersheath of the cable is given as follows

$$E_{is} = \omega\times I\times M_s \tag{3.13}$$

The induced current (I_{is}) in the Intersheath of the cable is given by the following expression

$$I_{is} = \frac{E_{is}}{\sqrt{\left(R_s^2 + \omega^2 M_s^2\right)}} \tag{3.14}$$

$$I_s = \frac{\omega\times I\times M_s}{\sqrt{\left(R_s^2 + \omega^2 M_s^2\right)}} \tag{3.15}$$

$\therefore$ Intersheath power loss (P_{is}) in the cable is given below

$$P_{is} = I_{is}^2\times R_s \tag{3.16}$$

$$P_{is} = \left(\frac{\omega^2 I^2 M_s^2}{R_s^2 + \omega^2 M_s^2}\right)\times R_s \tag{3.17}$$

Normally, sheath resistance $R_s >> \left(\omega\times M_s\right)$ such that

$$P_{is} = \frac{\omega^2 I^2 M_s^2}{R_s} \tag{3.18}$$

The sheath losses are smaller than the intersheath losses i.e. intersheath losses are larger and may vary from 10% to 50% of Copper (Cu) losses. Hence the total power loss (excluding dielectric loss) in the cable is given below

$$\text{Total power loss } (P_T) = P_{con} + P_s + P_{is}$$

$$P_T = \left(I^2 \times R_{con}\right) + \left(I^2 \left[\frac{3\omega^2}{R_s} \left(\frac{R_m}{d_c} \right)^2 \times 10^{-18} \right] \right) + \left(\frac{\omega^2 I^2 M_s^2}{R_s} \right) \tag{3.19}$$

Since, the expression is totally dependent on (I^2) and we may indicate the loss in terms of an effective resistance (R_E). Thus this provides the total loss of power in terms of an effective resistance is stated below

$$P_T = I^2 \times R_E$$

$$R_E = R_{con} + \left[\frac{3\omega^2}{R_s} \left(\frac{R_m}{d_c} \right)^2 \times 10^{-18} \right] + \left[\frac{\omega^2 M_s^2}{R_s} \right] \tag{3.20}$$

3.5 CROSS BONDING OF HV CABLES

When three 1-ϕ (single phase) cables are operated in the power transmission, currents are produced in the sheaths and this results in sheath circulating current and power loss in the cables. If these currents may be considerably decreased then the current rating of the cable is enlarged by cross-bonding of the cables.

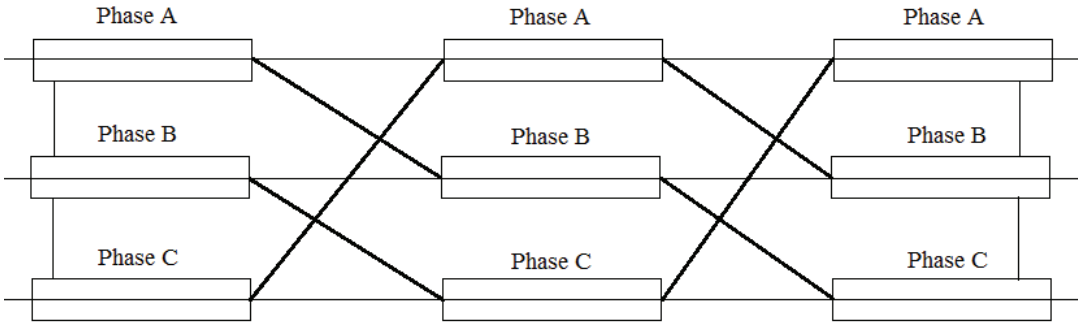

Figure 3.4 Cross bonding of the cable sheath

In general, the armour and sheath losses in 3-phase, 3-core cables are insignificant as of the symmetry configuration of the conductor. When separate three 1-core cables are employed, though, relatively great prolonged voltages are persuaded in each sheath of the cable, yet underbalanced conditions of the current, cause to unequal gaping of the sheaths comparative to any of the one conductor. These prolonged voltages cannot be abolished and hence if the sheaths are bonded in the normal scheme.

The stability of each sheath of the cable is broken at regular intervals of time, the cables between two nearby gaps being a trivial number of divisions. These small divisions make up a main section where the sheaths of the cables are steadily bonded together and to the earth.

A remaining sheath voltage in the core of the cable occurs and the preferred balance offering minor sheath voltage between the compact grounded spots which is achieved by interchanging the cables at the section of each cross-bonding of the sheaths. The following cable is interchanged as follows.

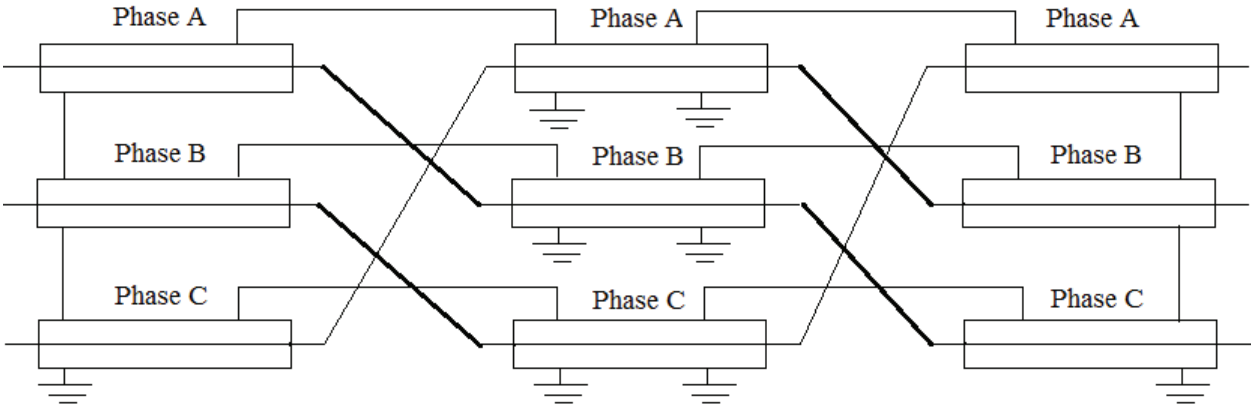

Figure 3.5 Non-linear resistor earthing

Mainly during the time of faults, to prevent from uncontrolled voltage formed at the cross bonded spots, these spots are earthed by non-linear resistors which restrict the uncontrolled voltage [17].

3.6 THERMAL CHARACTERISTICS OF CABLES

Thermal characteristics of the cables mainly depend upon two parameters and these two parameters are as follows

a) Thermal resistance of the cable.
b) Current rating of the cable.

3.6.1 THERMAL RESISTANCE OF THE CABLE

It may be stated as the thermal resistance which allows a heat flow of one watt when the temperature difference of $1^{\circ}C$ is kept maintained. Thermal resistance is measured in thermal ohms.

Let $'k'$ be the insulation thermal resistivity and as per similarity with the insulation resistance, the thermal resistance of a single core cable will be given as under

$$S_i = \frac{k}{2\pi l} ln\left(\frac{D_i}{d_i}\right) \text{ thermal ohms} \tag{3.21}$$

The value of thermal resistivity of the insulation is 750 for cables up to 2200 volts and 550 for cables above 2200 volts [18]-[19]

3.6.2 CURRENT RATING OF THE CABLE

When the values of thermal resistances are known then the current rating of a cable is governed. When the cable handles an excessive current, the cable gets heated up. Therefore, it is not suitable to operate the cable at extremely high temperature because of the following causes.

1. Oil in the oil-filled cables may cause the oil to be expanded due to high temperature and it results in bursting of the sheath of the cable.
2. At higher temperature, the viscosity of the oil decreases and leakage may start from higher levels.
3. Unequal expansion of the oil due to high temperature can cause formation of voids in the insulation which may lead to the ionization and lastly results to the failure of insulation.

4. Dielectric losses increase with the increase in temperature which may lead to the insulation breakdown. Therefore, the cable must be operated at a current less than the maximum handling current ability of the cable.

The current rating of a cable is dependent upon the following aspects

a) Maximum permissible temperature at which insulation of the conductor can be worked.
b) Heat dissipation configuration throughout the cable.
c) Atmospheric conditions at the time of installation.

The current carrying capacity of the cable is determined by the following equations:-

Let $n \rightarrow$ Number of cores

$R_{con} \rightarrow$ Resistance of the conductor in ohms per metre at $65^{\circ}C$

$I \rightarrow$ R.M.S. current value in amperes

$S_d \rightarrow$ Thermal resistance of the cable dielectric

Hence, nI^2R_{con} is the total core loss. The heat produced in the cable core passes through the dielectric medium to sheath of the cable.

We assume that $\phi_m \rightarrow$ Maximum tolerable temperature of the cable core

$\phi_s \rightarrow$ Temperature of the sheath

Then $$nI^2R_{con} = \frac{\phi_m - \phi_s}{S_d} \qquad (3.22)$$

Let γ = sheath loss/core loss

Therefore sheath loss = $\gamma \times$ core loss

Hence, Total loss = sheath loss + core loss

= $\gamma \times$ core loss + core loss

$$= (\gamma + 1) \text{ core loss}$$

Or simply, $\text{Total loss} = (1 + \gamma) \text{ core loss}$

$$\text{Total loss} = (1 + \gamma)\ nI^2 R_{con} \tag{3.23}$$

Above expression is the total heat flowing through bedding, serving and ground. The total thermal resistance of the bedding, serving and ground is given by '$S_b + S_s + G$' and the equivalent temperature difference is defined as the difference between sheath temperature (ϕ_s) and the ambient temperature (ϕ_a).

Therefore
$$(1+\lambda)nI^2 R_{con} = \frac{\phi_s - \phi_a}{S_b + S_s + G} \tag{3.24}$$

Normally 'ϕ_s' is not known then eliminate ϕ_s

$$\phi_m - \phi_s = nI^2 R_{con} S_d \tag{3.25}$$

$$\phi_s - \phi_a = (1+\lambda)nI^2 R_{con}(S_b + S_s + G)$$

$$\phi_m - \phi_a = nI^2 R_{con}\left[S_d + (1+\lambda)(S_b + S_s + G)\right] \tag{3.26}$$

$$I^2 = \frac{\phi_m - \phi_a}{nR_{con}\left[S_d + (1+\lambda)(S_b + S_s + G)\right]} \tag{3.27}$$

$$I = \sqrt{\frac{\phi_m - \phi_a}{nR_{con}\left[S_d + (1+\lambda)(S_b + S_s + G)\right]}} \tag{3.28}$$

Hence, this is the required expression used to determine the current carrying capacity of the cable [20].

CHAPTER 4

CONVERSION SCHEME

4.1 REPRESENTATIONOF BLOCK DIAGRAMFOR RESISTANCETO FREQUENCYAND DUTY-CYCLE CONVERSION

The block diagram consists of various electronic components such as integrated circuits, variable resistors and active low pass RC filter etc. The primary variable resistor is used for variation in frequency output and the secondary variable resistor is used for duty-cycle variation. The hysteresis comparators output feedback is used as input to the frequency varying sensor (Primary variable resistor) and to the operational amplifier based on a rectifier [22]-[24]. The basic block diagram for resistance to frequency converter is shown in figure 4.1:

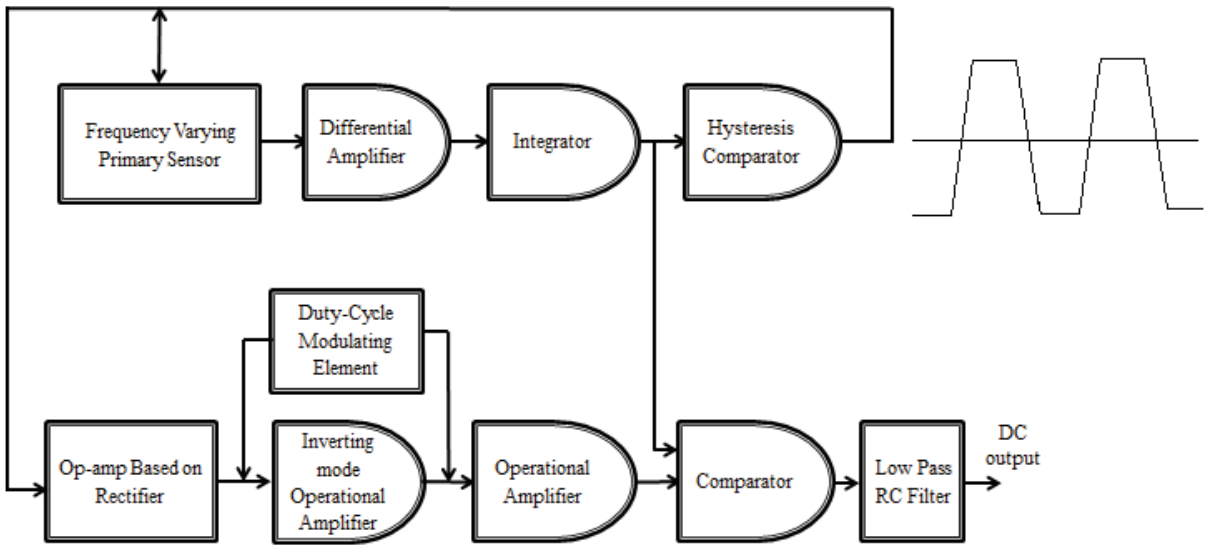

Figure 4.1 A basic block diagram of conversion scheme

A comparator compares the two voltages applied at the inputs and gives the digital output which is more. It has two input terminals i.e. are non-inverting input (plus) and inverting (minus) input. If the plus input is greater than the minus input then the output is high and if the plus input is

smaller than the minus input then the output is low. It is a special type of high gain differential amplifier. At last the duty-cycle output is converted into a DC analog signal by using the low pass RC filter at the comparators output.

4.2 SCHEMATIC DIAGRAMFOR RESISTANCETO FREQUENCY CONVERSION

In this conversion scheme, modeling of a resistance to frequency conversion is done. The converter is working on the principles of an electronic relaxation oscillator that generates a repetitive non-sinusoidal output signal such as a pulse width modulated (PWM) wave or a square wave or a triangular wave [25]. The oscillator circuit involves a feedback path having amplifying and switching device such as an operational amplifier, transistor, hysteresis comparator, comparator and a diode which charges a capacitor repetitively through resistance till it reaches near a threshold value and then it discharges again. The relaxation oscillators are normally employed for those signals having low frequency in various digital circuits. These types of oscillators are also used as voltage controlled oscillators (VCOs), analog-to-digital converters (ADCs) and also in function generators to generate square waves, triangular waves and pulse outputs. The schematic diagram for conversion scheme is shown in figure 4.2:

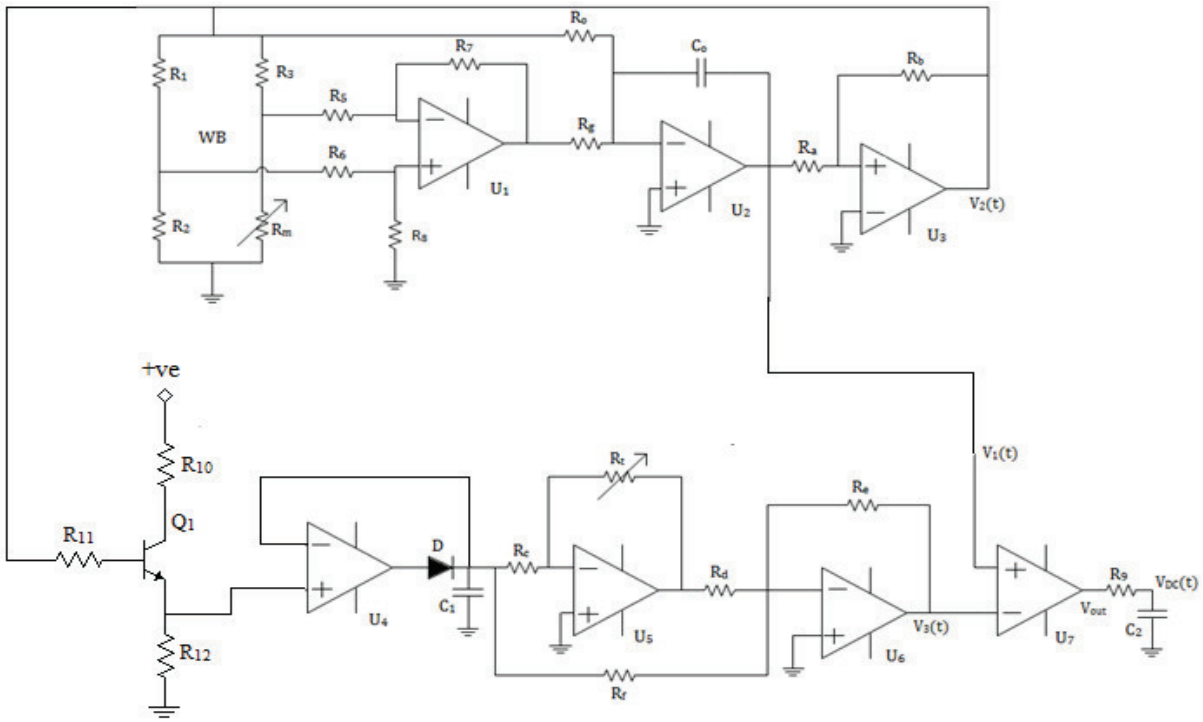

Figure 4.2 The schematic diagram of conversion scheme

4.3 EXPLANATIONOF EACH COMPONENTOFTHE SCHEMATIC DIAGRAM

In this portion, briefly explanation of each component used in the schematic circuit diagram will be discussed individually. The category and the connections of each component will also be deliberated.

4.3.1 WHEATSTONE BRIDGE

The resistors R_1, R_2, R_3 and R_m are configured in a Wheatstone bridge. The resistor R_m is a variable resistor whose change in percentage of resistance value changes the frequency. A Wheatstone bridge (R_1-R_m=11kΩ) is driven by the hysteresis comparators output voltage. The bridge unbalance factor is given by the following equation.

$$\lambda = \left(\frac{R_3}{R_1 + R_3} - \frac{R_m}{R_2 + R_m} \right) \tag{4.1}$$

Where 'λ' is the unbalance factor of the Wheatstone bridge.

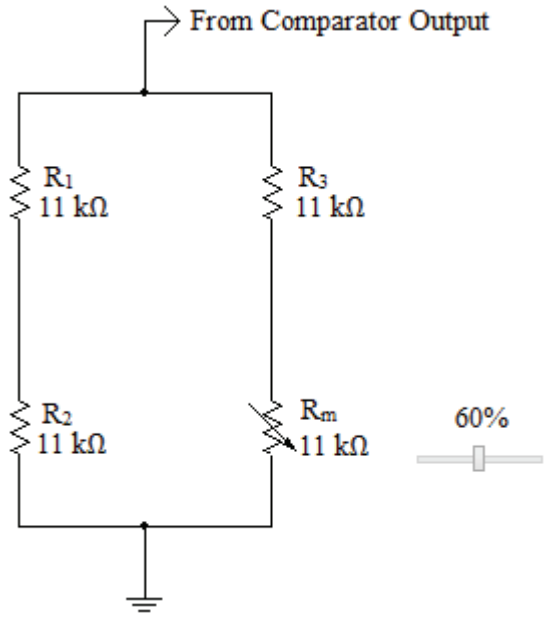

Figure 4.3 The arrangement of Wheatstone bridge

4.3.2 DIFFERENTIAL AMPLIFIER

An operational amplifier LM741CN is used as a differential amplifier in this circuit. A Wheatstone bridge unbalance voltage is amplified by the gain of the differential amplifier (U1). This type of amplifier uses non-inverting and inverting inputs both at the same time with a one gain (G) to generate an output signal equivalent to the difference between the applied inputs. The differential amplifier having two inputs V_1 and V_2 and one output V_o which is directly proportional to the difference between the two input voltages. It is given by the following expression

$$V_o = G(V_1 - V_2) \tag{4.2}$$

Where 'G' is the gain of the differential amplifier. This output is given to the 2 number pin of the integrator.

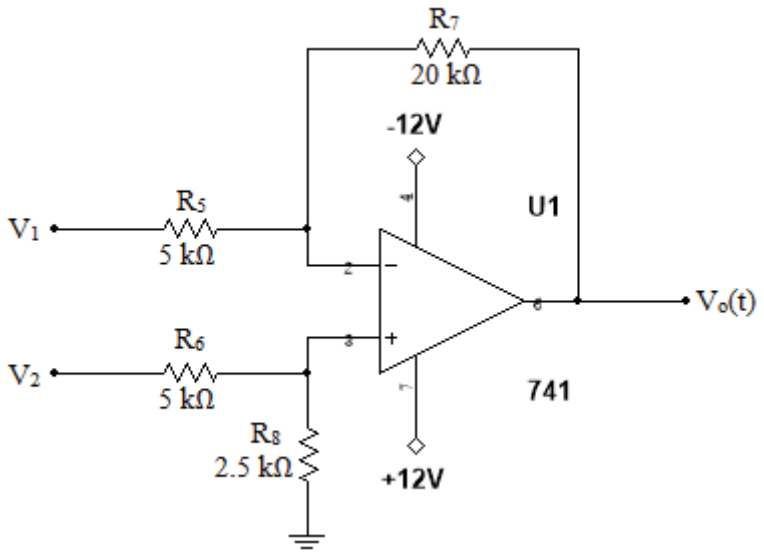

Figure 4.4 An IC 741 as a differential amplifier

4.3.3 INTEGRATOR

An integrator is a device in which the capacitor is used as a feedback component instead of a resistor on inverting input of the operational amplifier and the output signal corresponds to the time integral of its input signal. It executes the integration a part of mathematical operation with respect to the time i.e. the output signal voltage is proportional to the input signal voltage

incorporated over the time. It is most widely used in analog to digital converters (ADCs) and analog computers.

In this conversion scheme, the output waveform of an integrator is a triangular wave which is further applied as an input to the second comparator.

This triangular waveform of voltage $V_1(t)$ is attained with peak to peak amplitude by assuming V_{dd} or V_{ss} of hysteresis comparator (U3) as a symmetrical, hence $|V_{dd}| = |V_{ss}| = |V_s|$ which is given as under equation [26].

$$V_1 = 2V_s\left(\frac{R_a}{R_b}\right) \tag{4.3}$$

$$V_1(t) = -\frac{1}{R_oC_o}\int_0^{T/2} V_o(t)dt - \frac{1}{R_oC_o}\int_0^{T/2} V_2(t)dt \tag{4.4}$$

When the condition reached at which the bridge is to be balanced then $V_o(t) = 0$.

$$V_1(t) = -\frac{1}{R_oC_o}\left(\frac{T}{2}\right)\left(-V_s\right) \tag{4.5}$$

$$= \frac{1}{2}\left(\frac{V_sT}{R_oC_o}\right)$$

$$T = \frac{4C_oR_oR_a}{R_b} \tag{4.6}$$

Irrespective values of $V_1(t)$ and V_s with frequency ‘f ’ is given by the following equations.

$$f = f_o\left[1+\lambda G\frac{R_o}{R_g}\right] \tag{4.7}$$

Where 'f_o' is the center frequency.

$$f_o = \frac{R_b}{4C_oR_oR_a} \tag{4.8}$$

An op-amp 741 is worked as an integrator in this circuit and is shown in the fig-

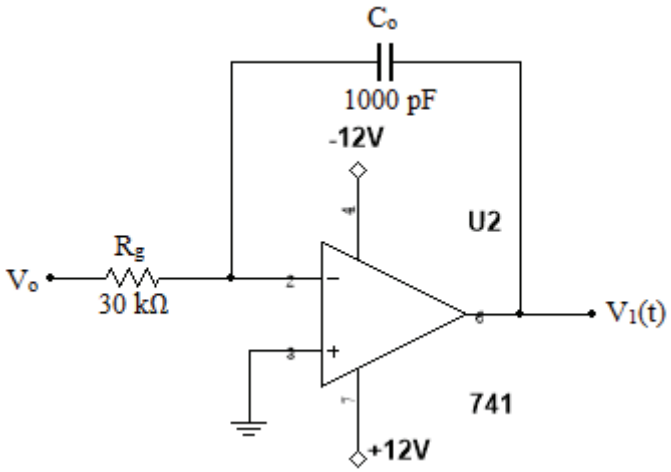

Figure 4.5 An IC 741 as an integrator

The output waveform of an integrator is shown below in the fig-

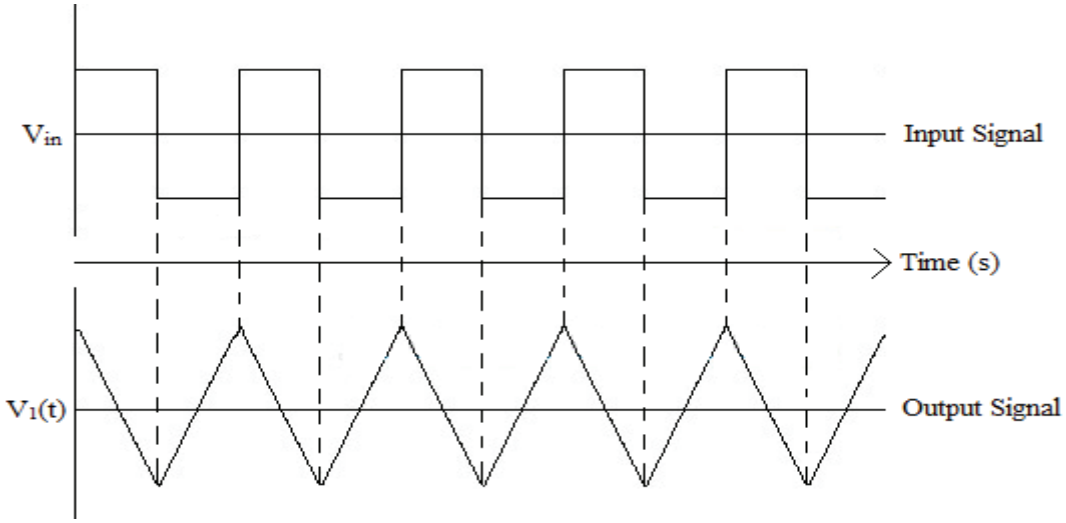

Figure 4.6 The input and output signal waveforms of an integrator

4.3.4 HYSTERESIS COMPARATOR

A hysteresis comparator is designed using op-amp 741 in this circuit. A comparator having both input resistor and feedback resistor value of 1 kΩ. The output voltage signal $V_2(t)$ is provided feedback signal as a input to the Wheatstone bridge.

$$V_d = V_{(+)} - V_{(-)} \tag{4.9}$$

$$= \frac{R_a}{R_a + R_b} V_2(t) + \frac{R_b}{R_a + R_b} V_1(t) - 0 \tag{4.10}$$

$$\frac{R_a}{R_a + R_b} V_2(t) + \frac{R_b}{R_a + R_b} V_1(t) = 0 \tag{4.11}$$

$$V_{th} = -\frac{R_a}{R_b} V_2(t) \tag{4.12}$$

Positive output state, $V_p = V_2(t)$ (4.13)

Negative output state, $V_n = V_2(t)$ (4.14)

An operational amplifier plays as a hysteresis comparator which gives the frequency. The arrangement of this comparator is shown in the figure.

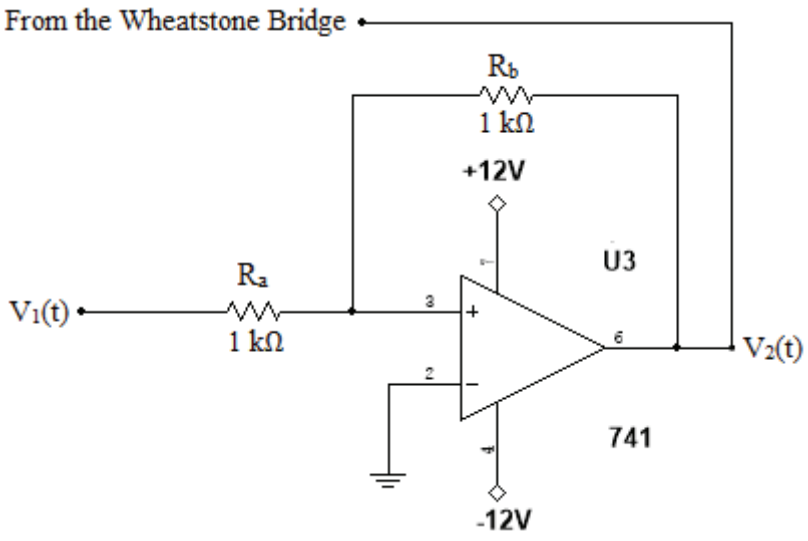

Figure 4.7 An IC 741 as a hysteresis comparator

4.3.5 TRANSISTOR

In this circuit, the voltage signal as an input from Wheatstone bridge is fed to the base terminal of the npn transistor. The arrangement of BC547 npn transistor in the circuit is given below in the figure 4.8.

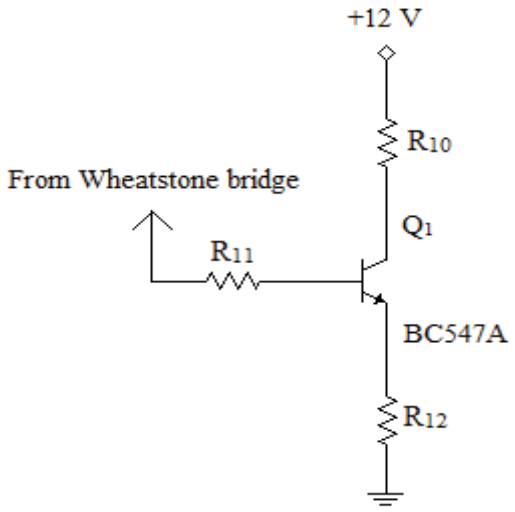

Figure 4.8 The arrangement of BC547 transistor

4.3.6 OP-AMPBASEDONARECTIFIER

An Op-amp 741 is used as an operational amplifier which is based on a rectifier and parallel with a capacitor of 650 pF.

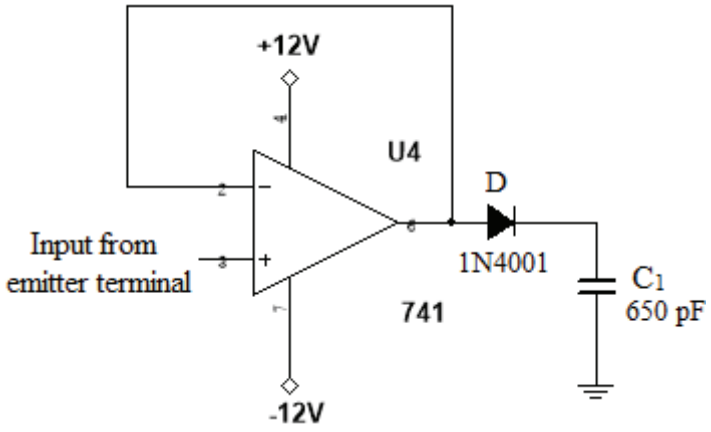

Figure 4.9 An op-amp based on a rectifier

4.3.7 OP-AMPBASEDONADUTY-CYCLEMODULATINGELEMENT

An inverting mode of op-amp 741 in which the duty-cycle modulating element or thermal resistive sensor or a variable resistor is connected in the feedback path. An operational amplifier across which the duty-cycle modulating element is to be connected in the feedback is shown below in the figure.

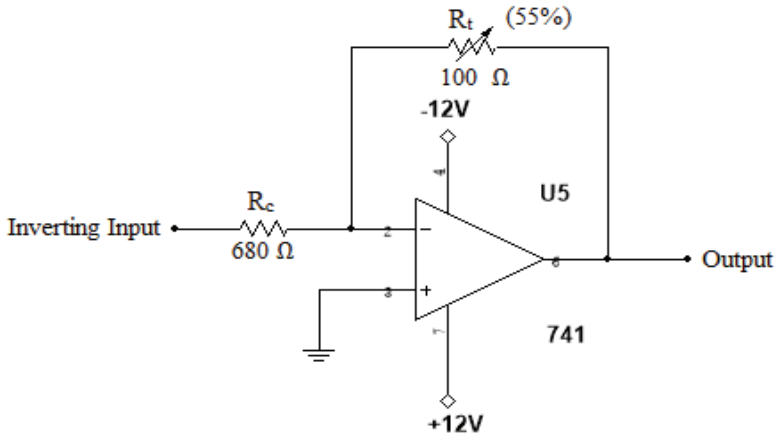

Figure 4.10 An op-amp based on the duty-cycle modulating element

4.3.8 INVERTING MODE OP-AMP 741

An Op-amp 741 has inverting input with feedback resistor and one output. The input resistor of this operational amplifier is connected to the previous op-amp across which the variable resistor is to be connected. The 3 number pin of this op-amp is to be grounded.

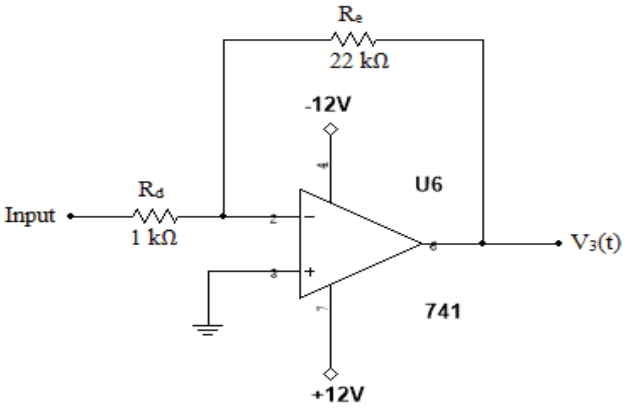

Figure 4.11 An inverting mode op-amp 741

4.3.9 COMPARATOR

The output of an integrator is a triangular waveform ($V_1(t)$) which is compared with earlier inverting mode op-amp output ($V_3(t)$) by the comparator (U7) whose output is $V_{out}(t)$.

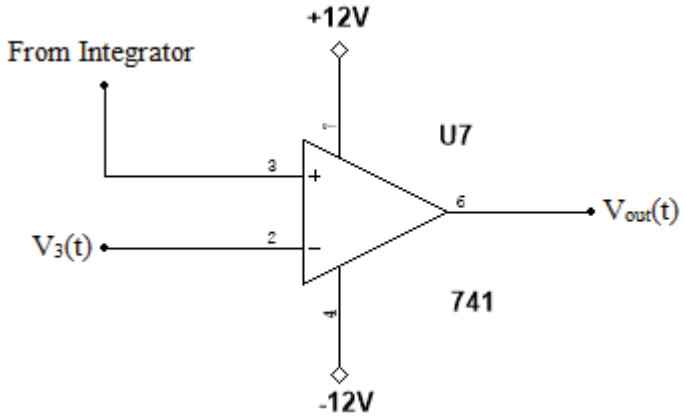

Figure 4.12 An IC 741 as a comparator

Thus the duty-cycle (dc) is defined as the ratio of one time period in which the signal is active to a time period in which the signal is active and inactive both that is T_{ON} / T, where T is T_{ON} + T_{OFF}. Hence, the expression for duty-cycle is given as under.

$$dc = \frac{1}{2}\left[1 - \frac{R_b}{R_a} R_e \left(\frac{R_t}{R_c R_d} - \frac{1}{R_f}\right)\right] \tag{4.15}$$

4.3.10 RC LOW PASS FILTER

Furthermore, duty-cycle (dc) of pulse width modulated (PWM) wave can be simply converted into analog DC signal by using RC low pass filter

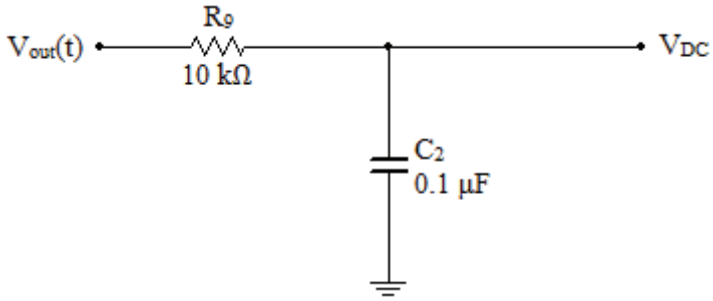

Figure 4.13 RC Low pass filter

CHAPTER 5

SIMULATION OF AN INTERFACING CIRCUIT

5.1 INTRODUCTION

An interfacing circuit is the circuit which permits one sort of circuit to be connected to another sort of circuit having a different current and voltage rating. In this, we can interface input devices such as sensors, transistors and diodes for switching purpose as well as output devices such as solenoids, lights and relays for linking together.

Therefore the interfacing of output devices to electronic and electrical circuits is commonly called output interfacing. In the field of control engineering, there are three types of stages that are done for interfacing circuit. First stage which is commonly used consist of sensor i.e. sensing stage, second stage is the signal conditioning stage in which usually amplification of the signal is done and third stage is a processing stage which is normally carried out by a microcontroller and an analog-to-digital converter (ADC). Operational amplifiers (Op-Amps) are commonly used to carry out the amplification of the signal in the second stage.

Here, I have designed a linear and sensitive Wheatstone bridge based interfacing circuit for condition monitoring of moisture content and temperature compensation in the trenches of high-voltage underground cables. In this circuit, Conversion of resistance in terms of frequency and duty-cycle is done. This circuit is based on the principles of relaxation oscillator. An interfacing circuit for two resistive sensors which is operated on a Wheatstone bridge for the transformation of incremental resistance into the frequency and the duty-cycle due to the change in moisture and temperature of the filler material of the HV underground cable at the same time convey the information from a pair of these resistive type sensors i.e. are impedance moisture sensor and the thermal sensor [27]-[30] It is simulated in NI Multisim 13.0 software with the help of inbuilt components and devices in this software as shown simulation model in the figure.

5.2 SIMULATION MODEL

The simulation model of an interfacing circuit is synthesized on NI Multisim software version 13.0. which is shown in the following figure. A Multisim simulation software is used to design the different types of circuits and to enhance the shorten period of time to prototype.

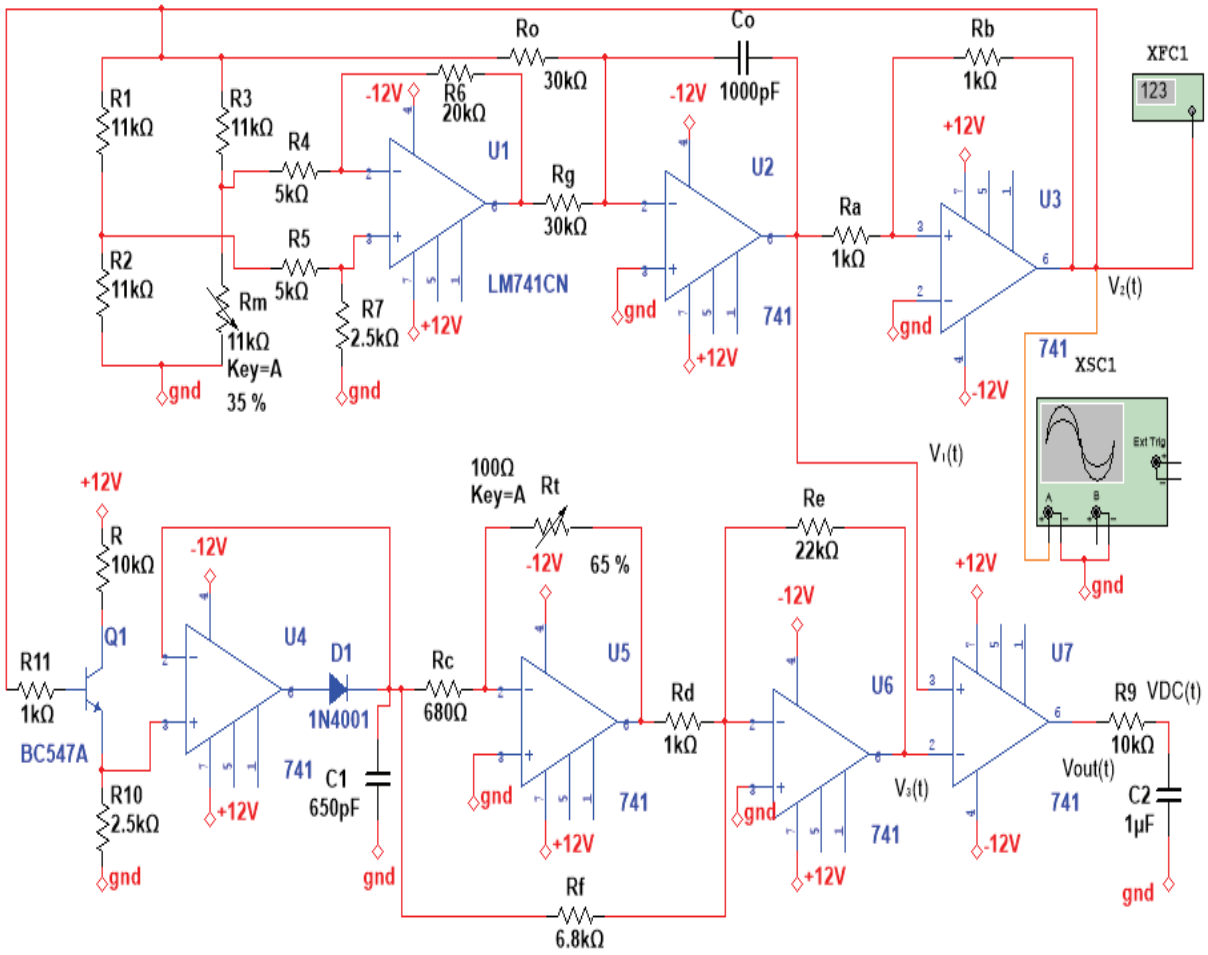

Figure 5.1 Simulation of circuit performed on a Multisim software

5.3 SIMULATION RESULTSON MULTISIM

The following are the simulated results and obtained on an oscilloscope at different terminals of output are described shown in the figures 5.2 – figures 5.17.

- **Simulated result of an integrator $V_1(t)$at R_m=20%**

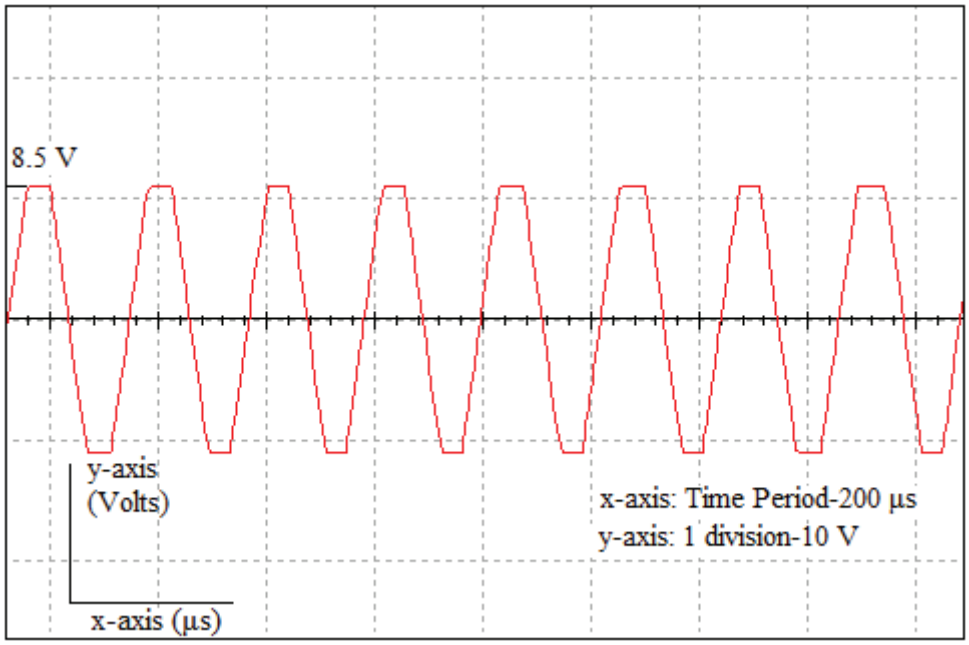

Figure 5.2 Output of an integrator at R_m=20%

- **Simulated result of integrator V1(t) at Rm=40%**

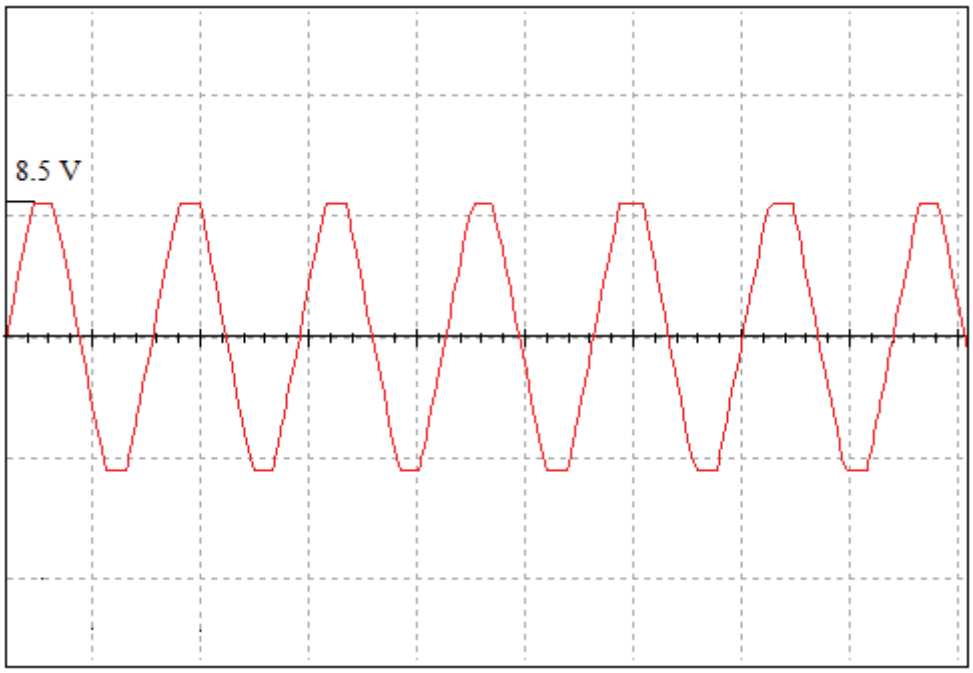

Figure 5.3 Output of integrator at R_m=40%

- **Simulated result of integrator $V_1(t)$ at R_m=60%**

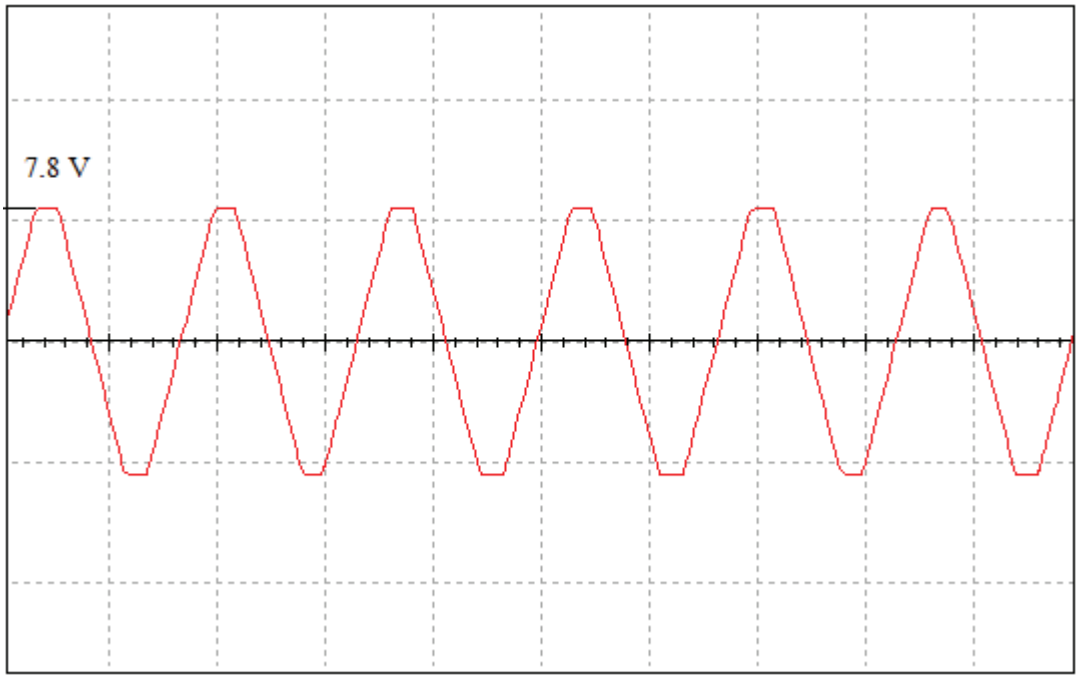

Figure 5.4 Output of integrator at R_m=60%

- **Simulated result of integrator $V_1(t)$ at R_m=80%**

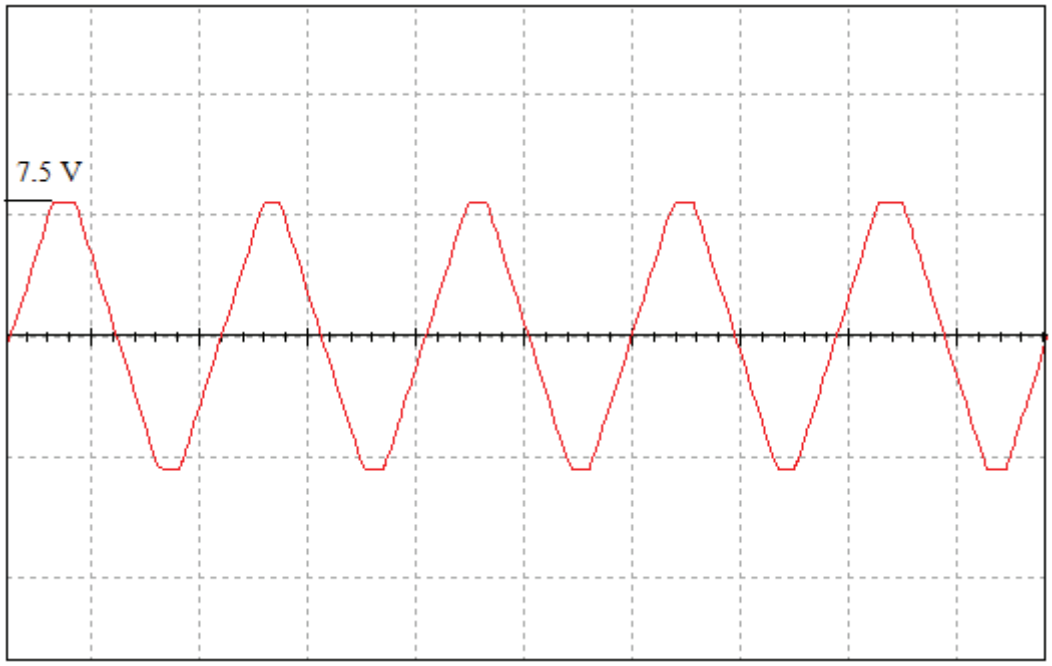

Figure 5.5 Output of integrator at R_m=80%

- **Simulated result of integrator $V_1(t)$ at R_m=100%**

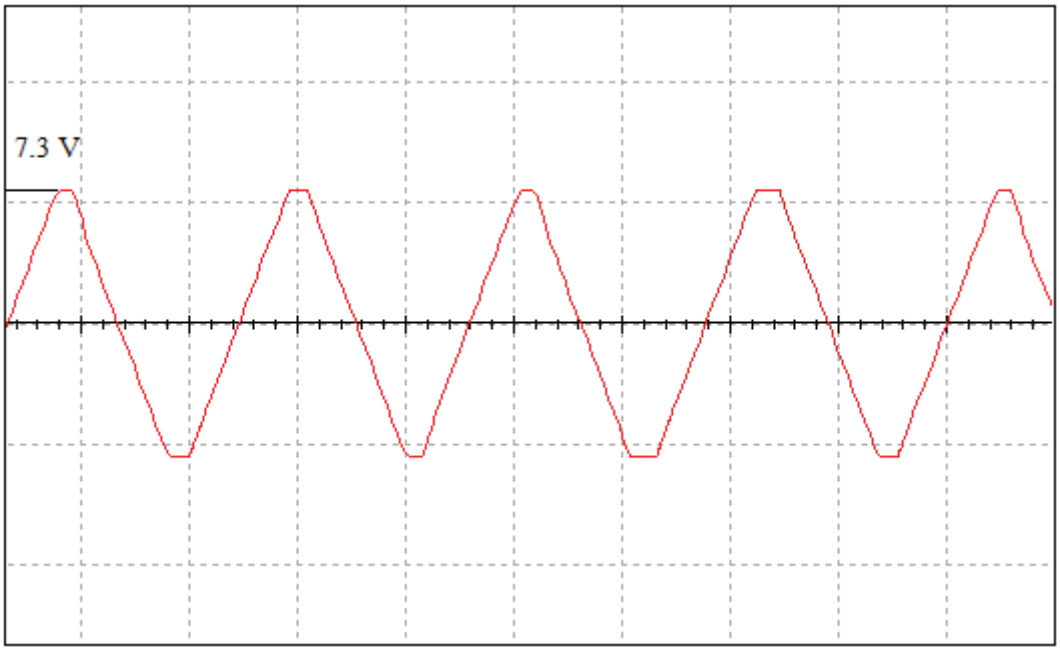

Figure 5.6 Output of integrator at R_m=100%

- **Simulated result of hysteresis comparator $V_2(t)$ at R_m=20%**

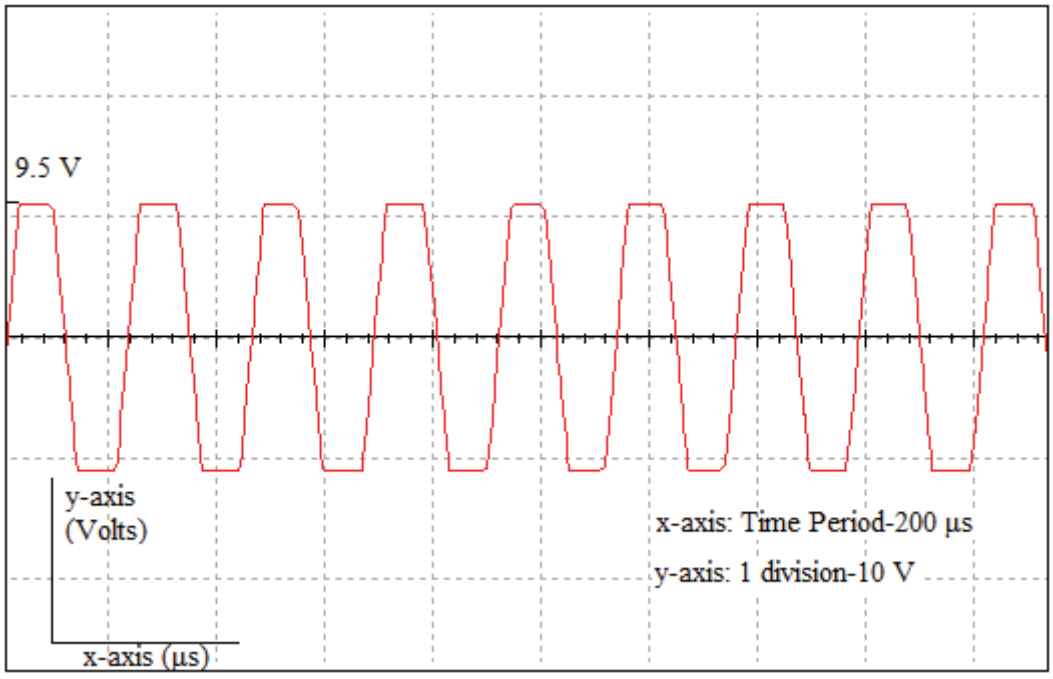

Figure 5.7 Output of hysteresis comparator at R_m=20%

- **Simulated result of hysteresis comparator $V_2(t)$ at R_m=40%**

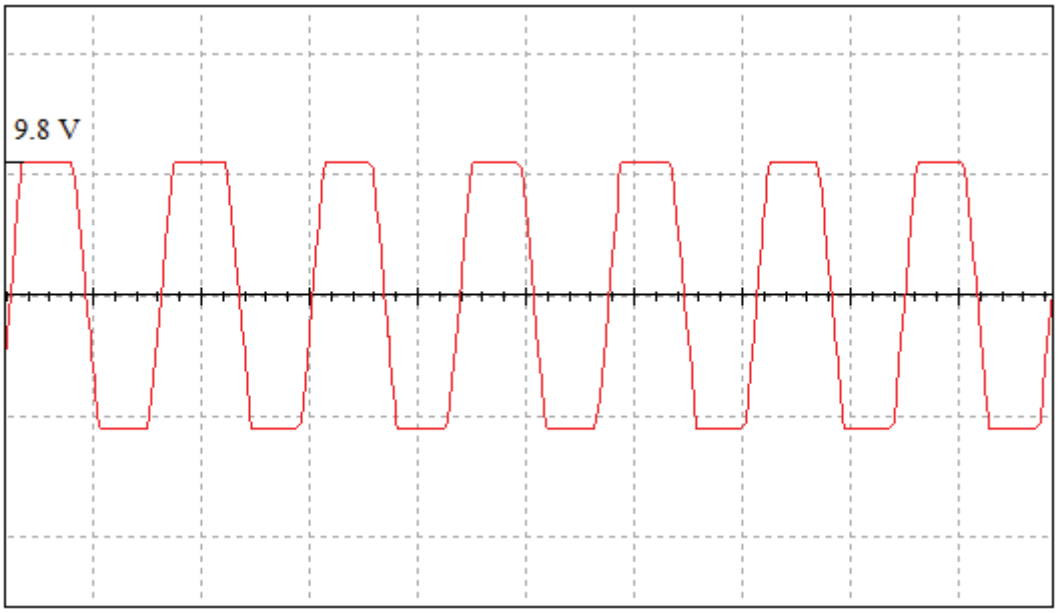

Figure 5.8 Output of hysteresis comparator at R_m=40%

- **Simulated result of hysteresis comparator $V_2(t)$ at R_m=60%**

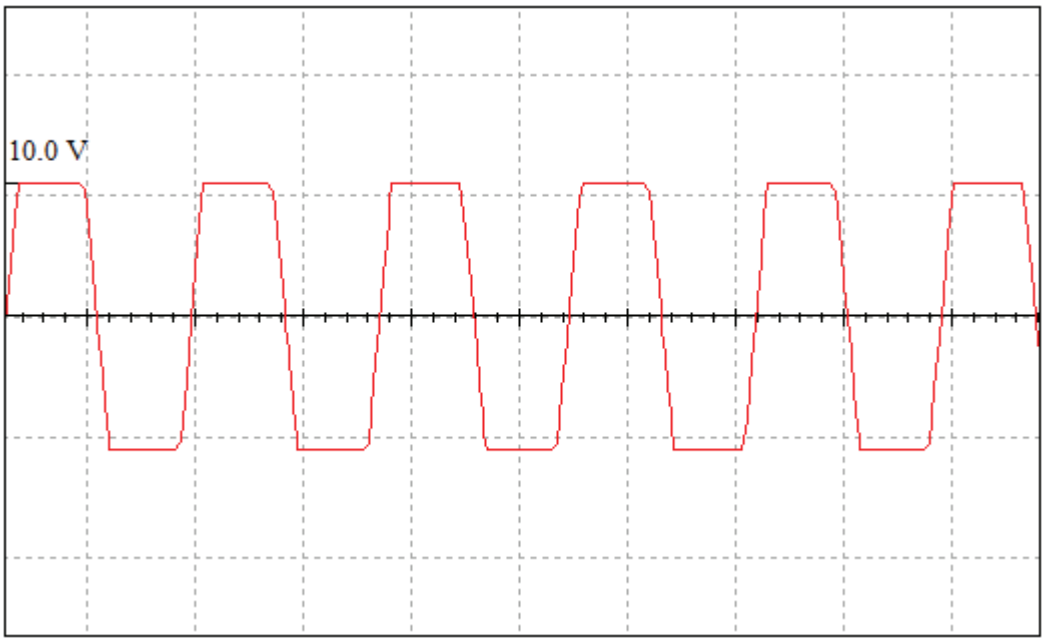

Figure 5.9 Output of hysteresis comparator at 60%

- **Simulated result of hysteresis comparator $V_2(t)$ at R_m=80%**

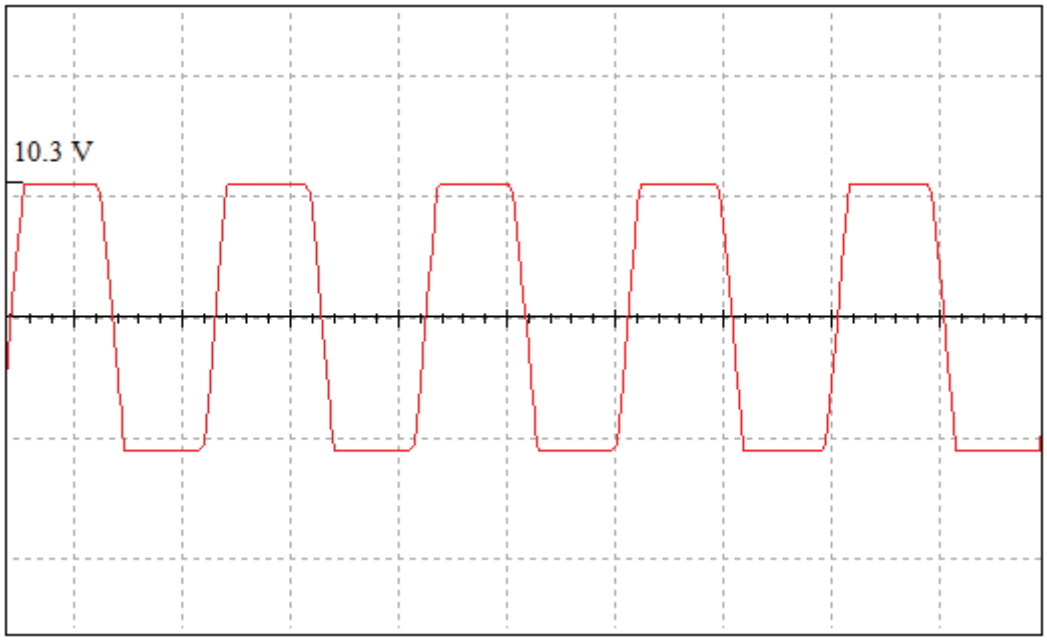

Figure 5.10 Output of comparator at 80%

- **Simulated result of hysteresis comparator $V_2(t)$ at R_m=100%**

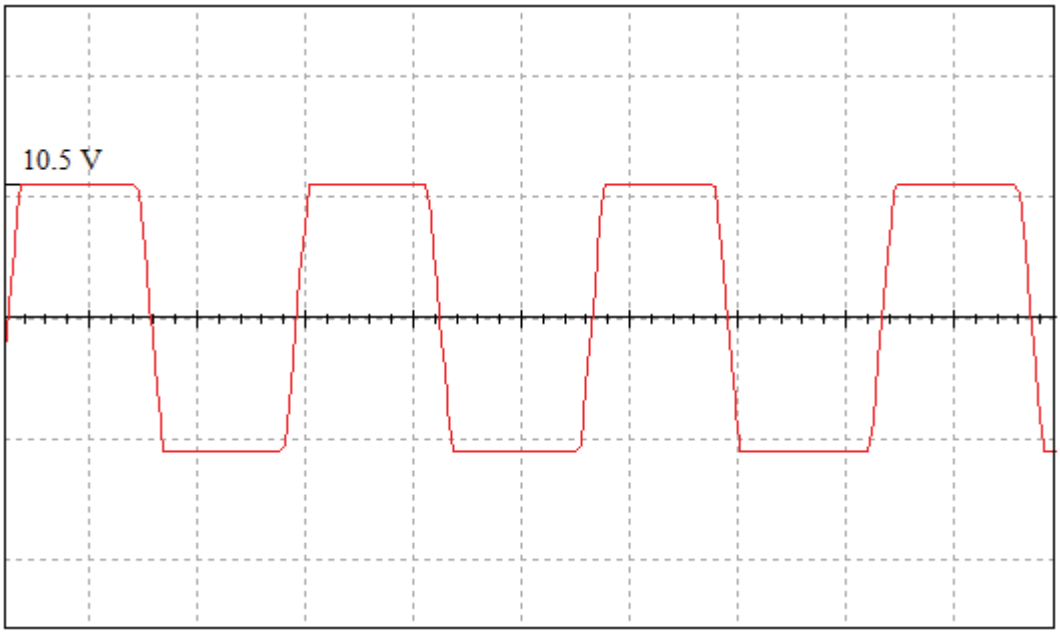

Figure 5.11 Output of hysteresis comparator at 100%

- **Simulated result of comparator $V_{out}(t)$ at R_m=20%**

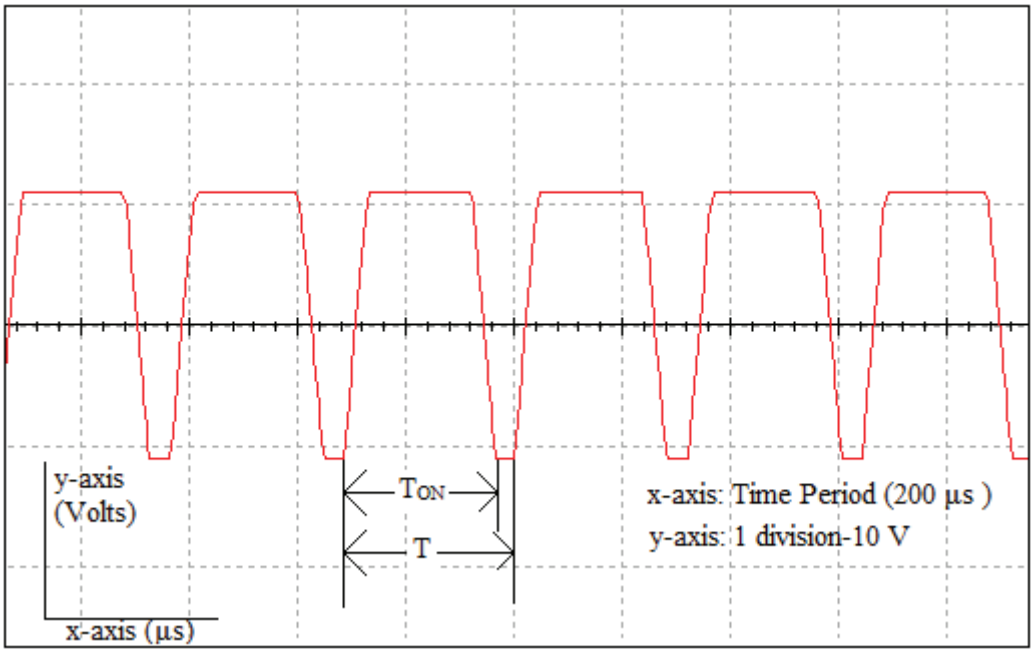

Figure 5.12 Output of comparator at R_t=20%

- **Simulated result of comparator $V_{out}(t)$ at R_m=40%**

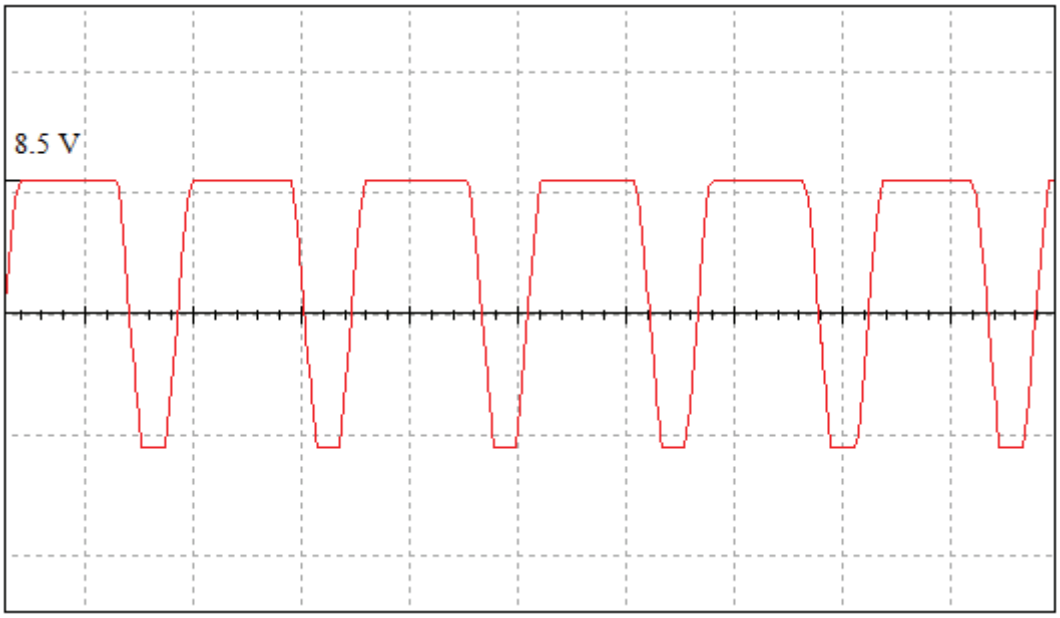

Figure 5.13 Output of comparator at R_t=40%

- **Simulated result of comparator $V_{out}(t)$ at R_m=60%**

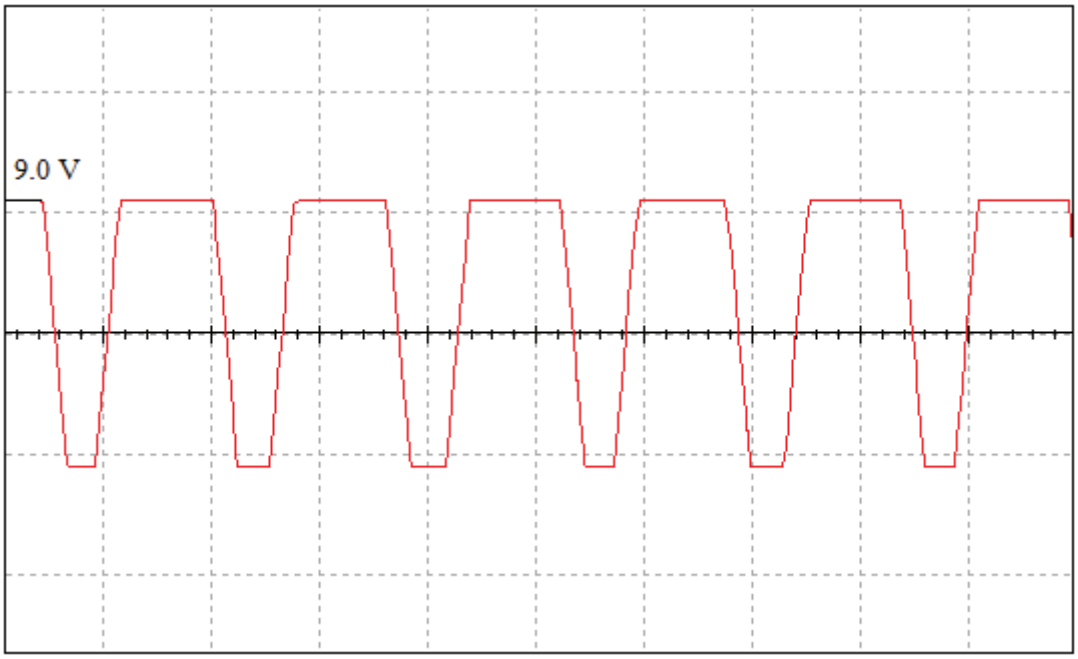

Figure 5.14 Output of comparator at R_t=60%

- **Simulated result of comparator $V_{out}(t)$ at R_m=80%**

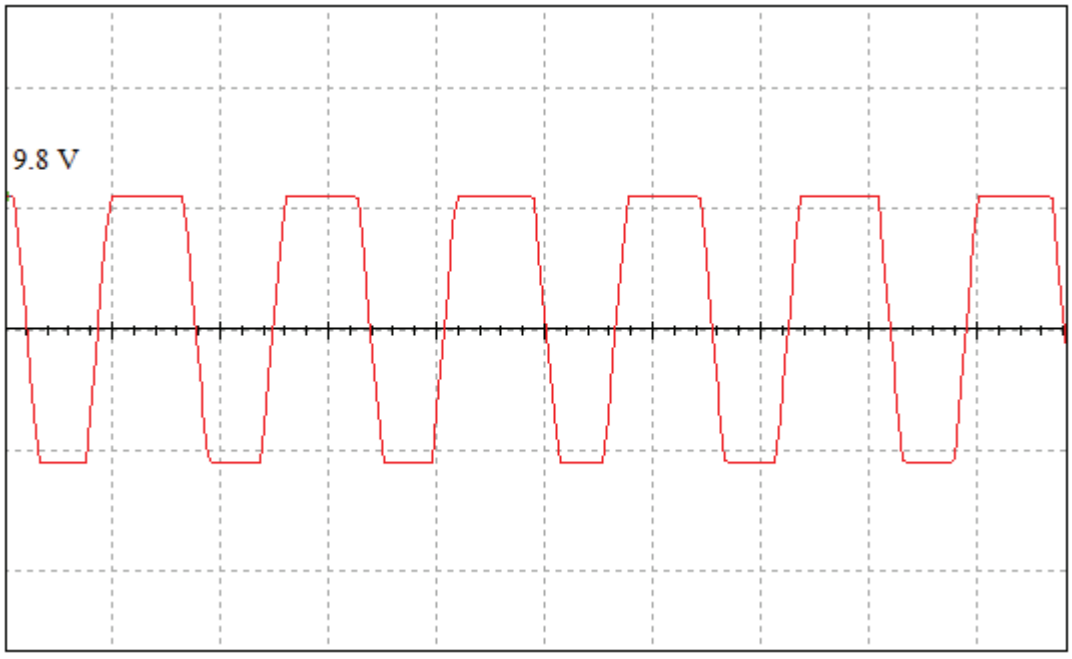

Figure 5.15 Output of comparator at R_t=80%

- **Simulated result of comparator $V_{out}(t)$ at R_m=100%**

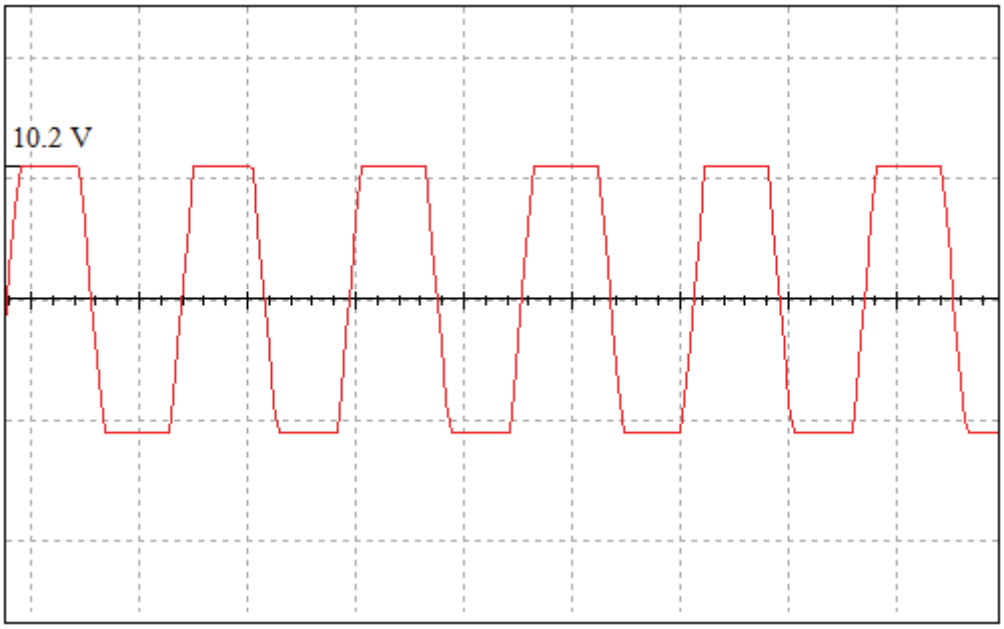

Figure 5.16 Output of comparator at R_t=100%

- **Simulated result after RC low pass filter**

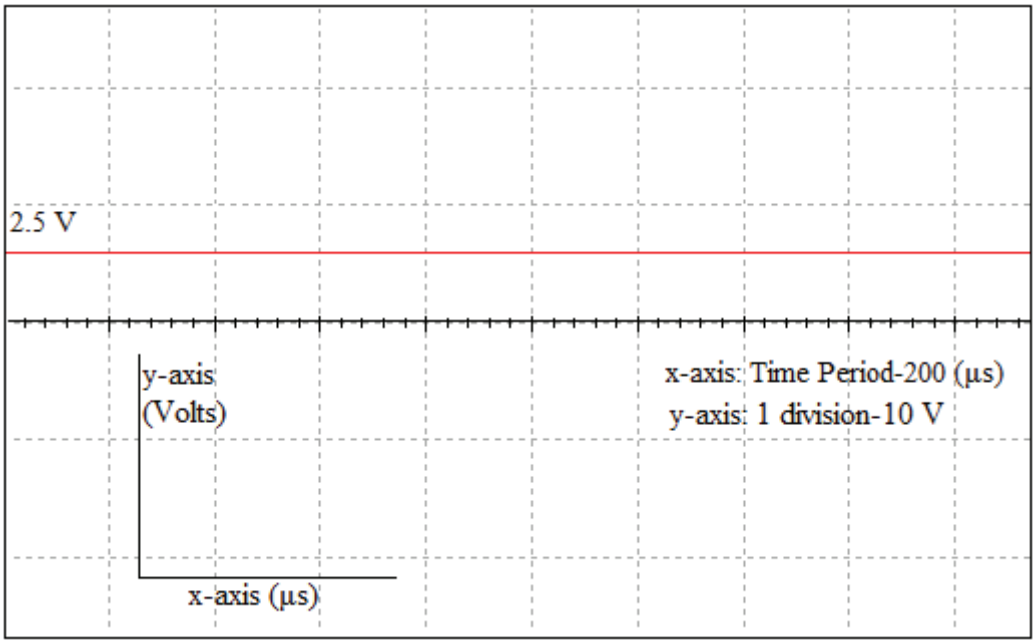

Figure 5.17 DC Output after low pass filter

5.4 EXPERIMENTAL SETUP OF AN INTERFACING CIRCUIT

The experimental setup of an interfacing circuit is to be done on a breadboard for hardware implementation. The experimental output results at different steps are captured on a cathode ray oscilloscope (CRO).

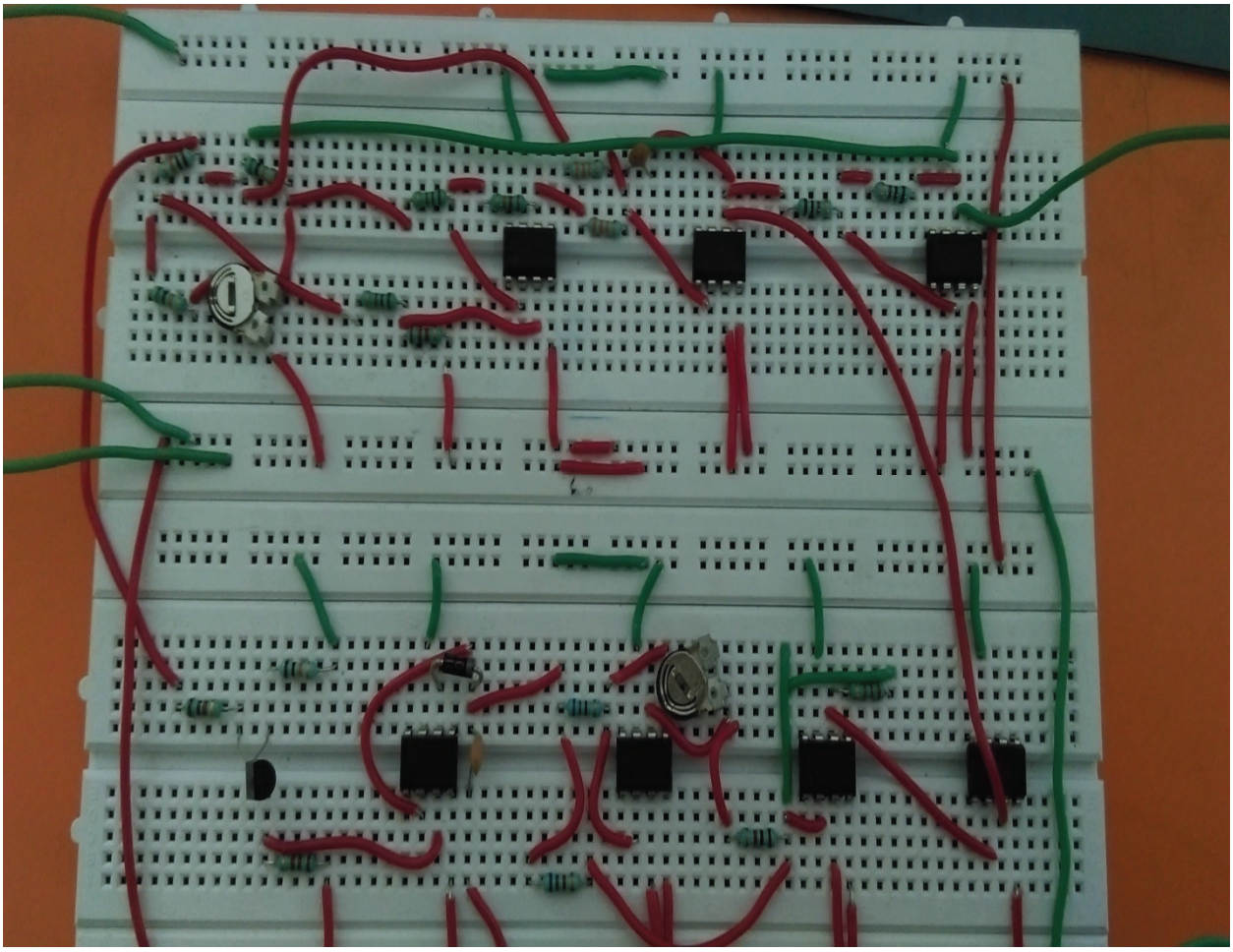

Figure 5.18 Interfacing circuit implemented on a breadboard

5.5 EXPERIMENTAL RESULTS

The output result of the integrator is obtained at oscilloscope (CRO) is deliberated in the following figures 5.19 - figures 5.27:

- **Experimental output of integrator$V_1(t)$ at R_m=20%**

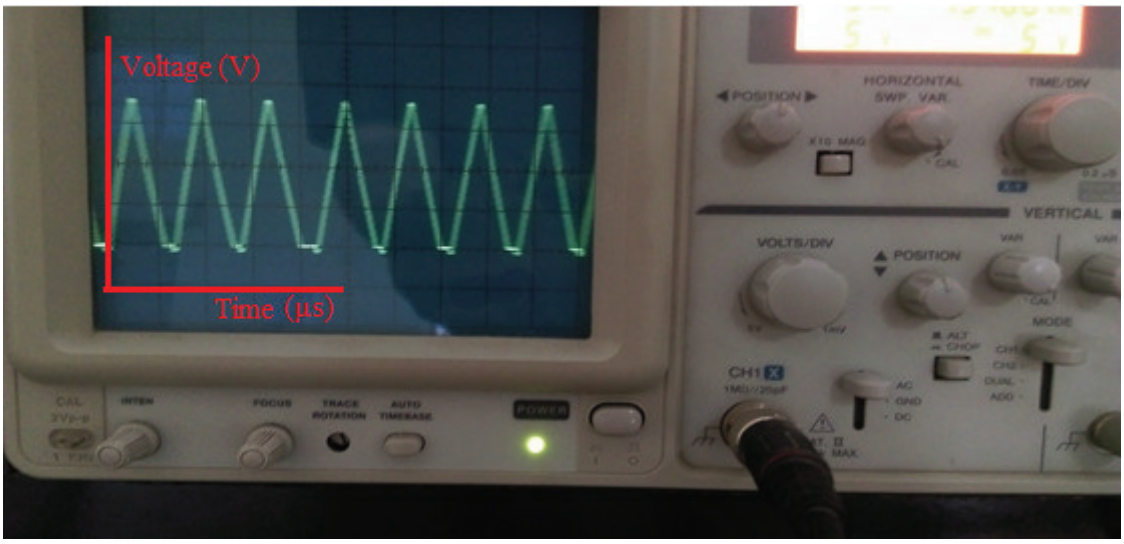

Figure 5.19 Output of integrator when R_m=20%

- **Experimental output of integrator $V_1(t)$ at R_m=20%**

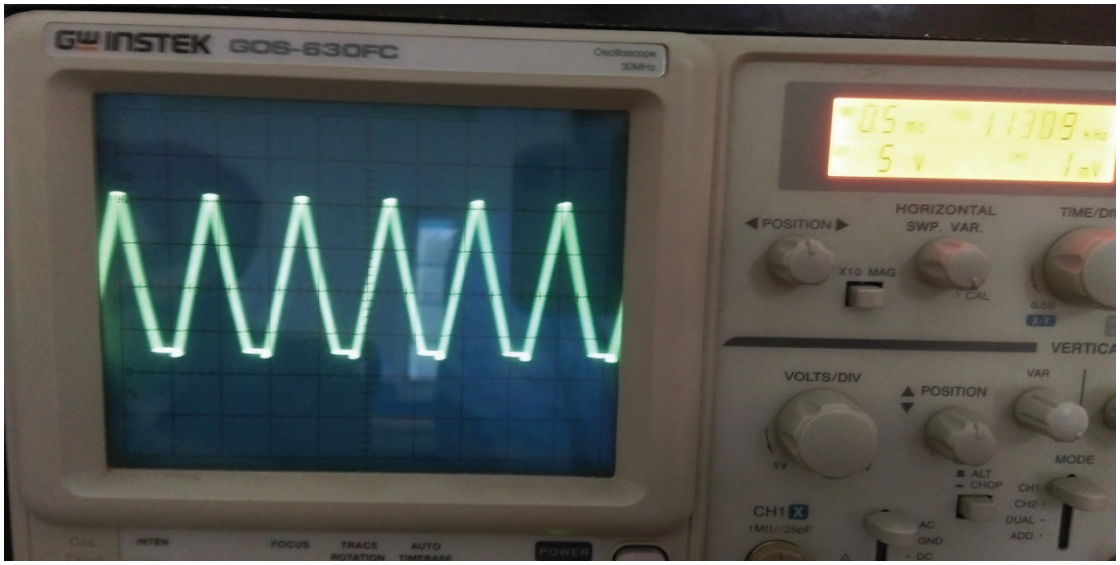

Figure 5.20 Output of integrator when R_m=60%

- **Experimental output of integrator $V_1(t)$ at R_m=20%**

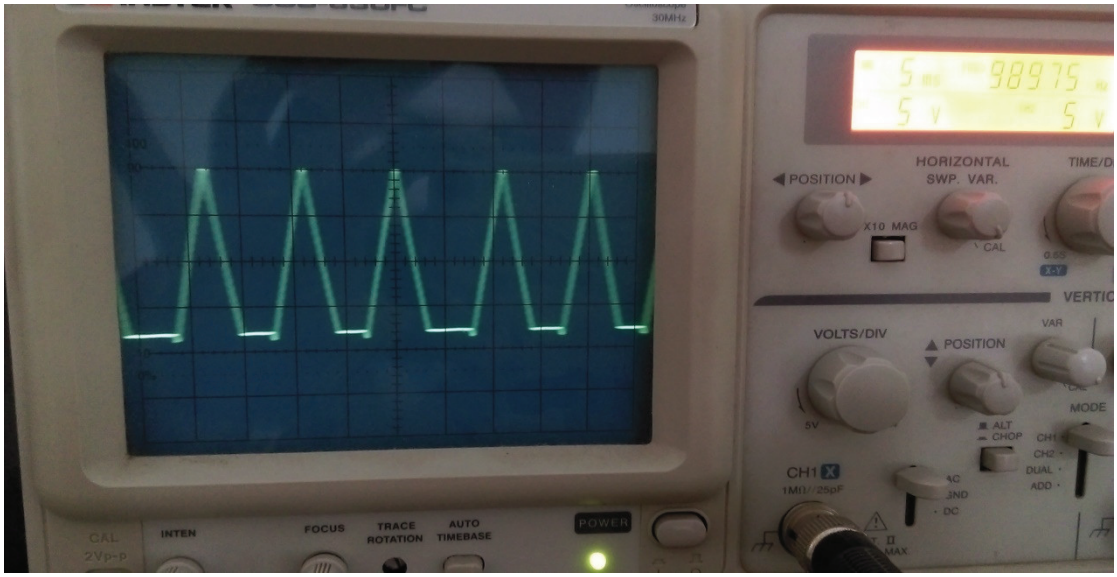

Figure 5.21 Output of integrator when R_m=100%

- **Experimental output of hysteresis comparator $V_2(t)$ at R_m=20%**

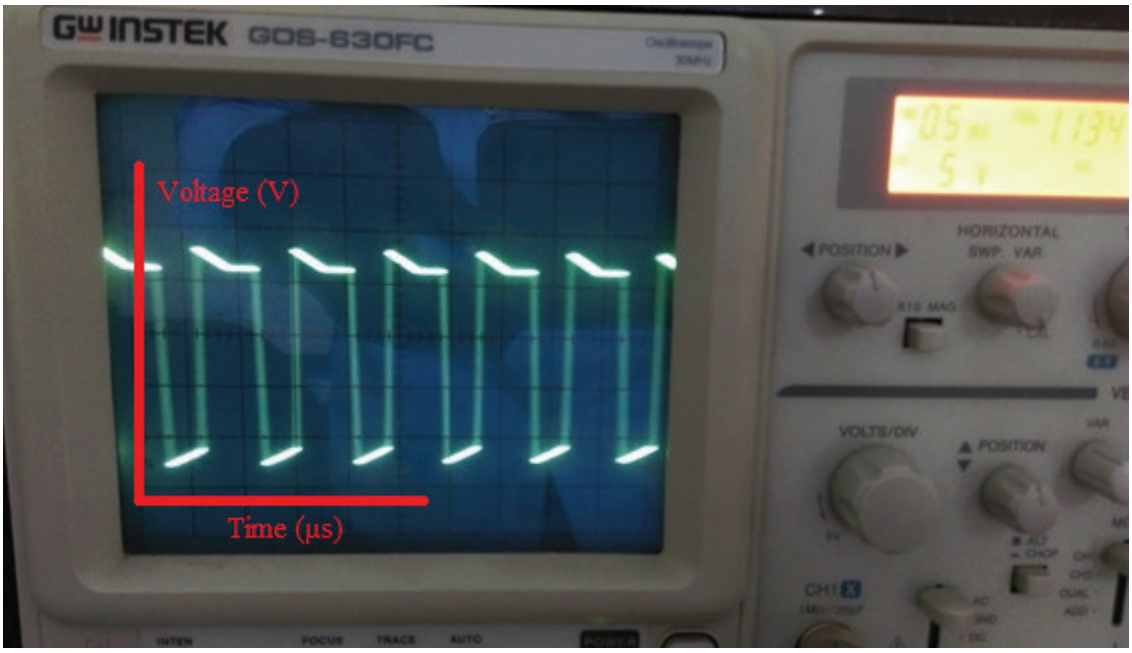

Figure 5.22 Output of hysteresis comparator at R_m=20%

- **Experimental output of hysteresis comparator $V_2(t)$ at R_m=60%**

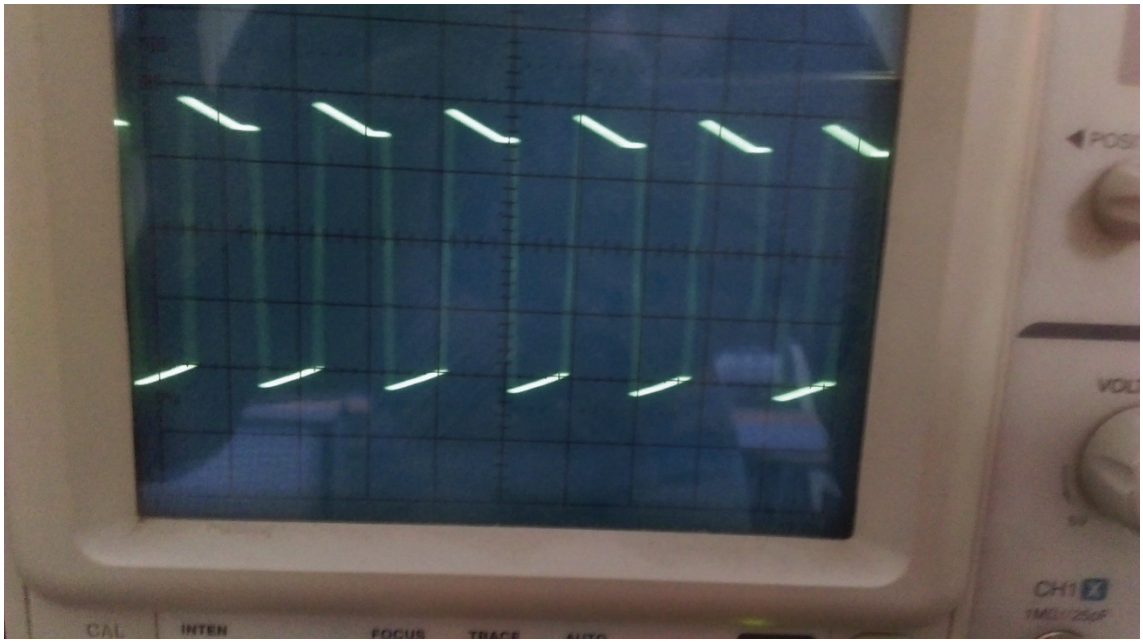

Figure 5.23 Output of hysteresis comparator at R_m=60%

- **Experimental output of integrator $V_1(t)$ at R_m=100%**

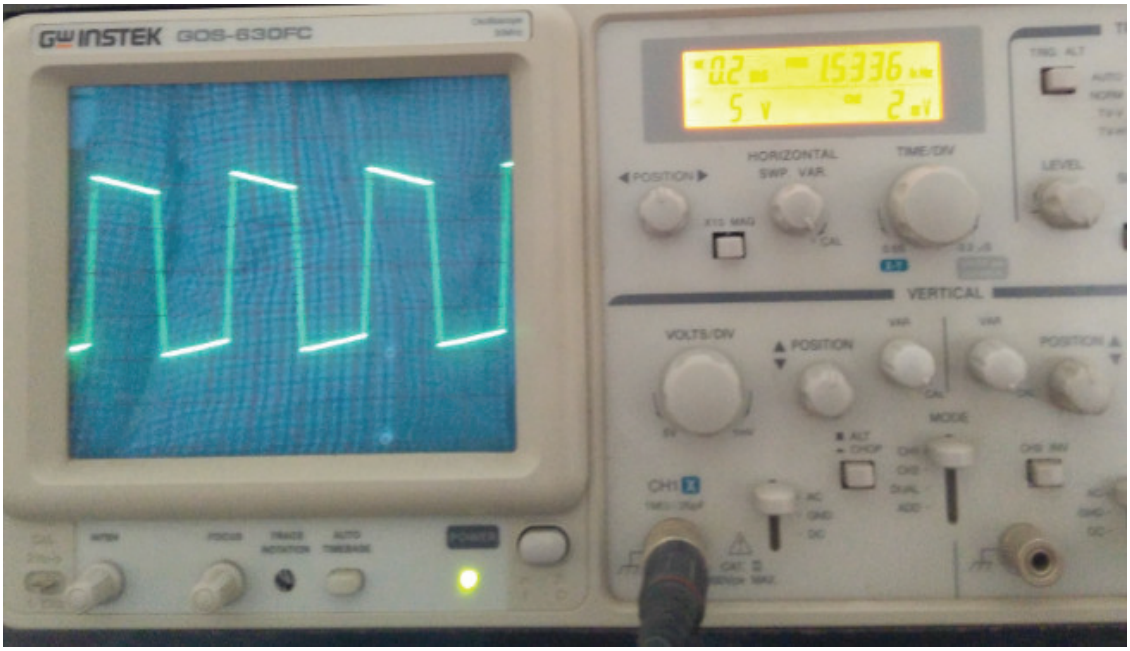

Figure 5.24 Output of hysteresis comparator at R_m=100

- **Experimental output of comparator $V_{out}(t)$ at R_m=20%**

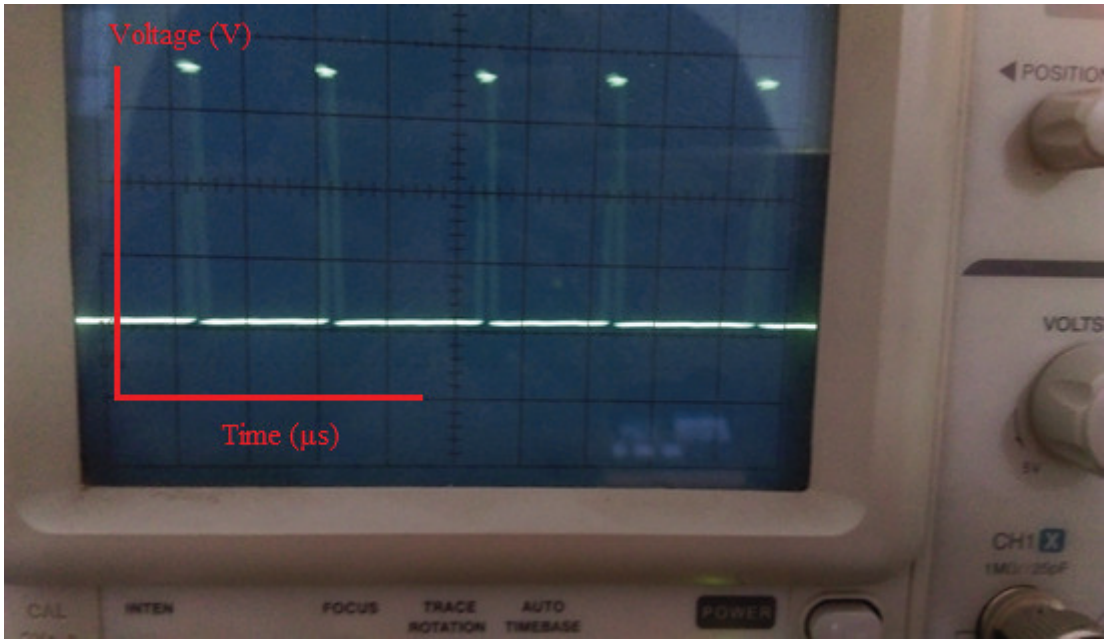

Figure 5.25 Output of comparator at 20%

- **Experimental output of comparator $V_{out}(t)$ at R_m=60%**

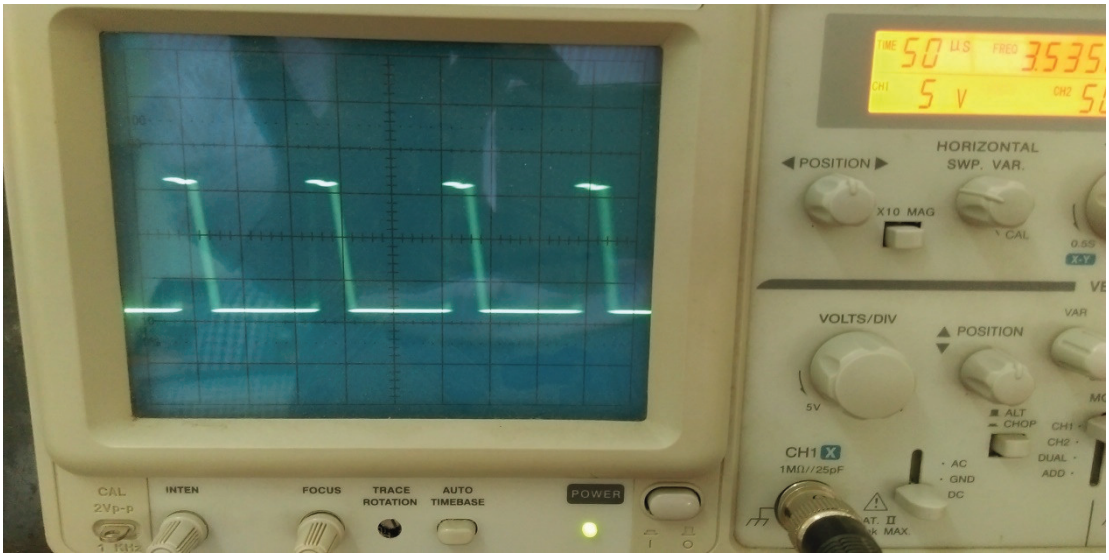

Figure 5.26 Output of comparator at R_t=60%

- **Experimental output of comparator $V_{out}(t)$ at R_m=100%**

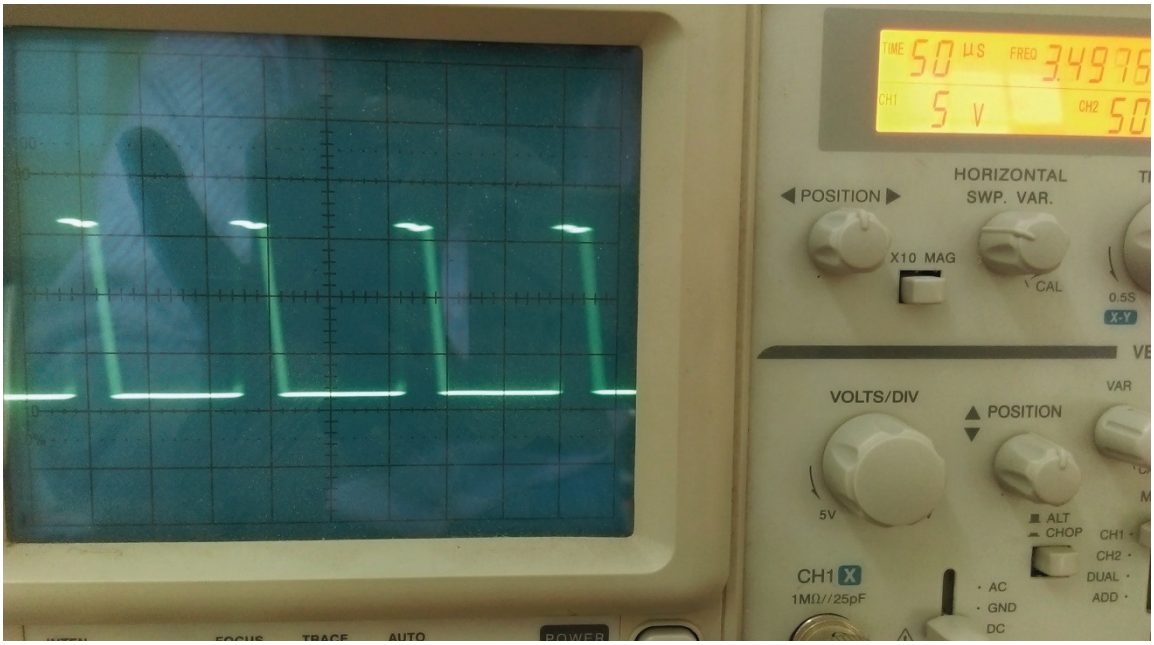

Figure 5.27 Output of comparator at R_t=100%

5.6 GRAPHICAL REPRESENTATION OF OUTPUT RESULTS

- **The graph drawn between frequency and change in resistance to the original resistance (ΔR/R) at different values**.

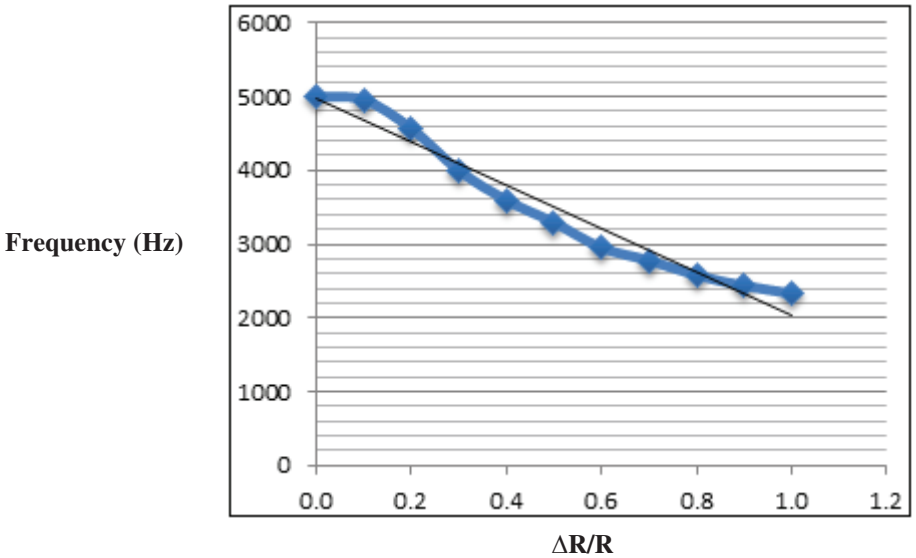

Figure 5.28 Graphical representation of output frequency with ΔR/R

- **The graph drawn between the duty-cycle and change in thermal resistance (R_t)**

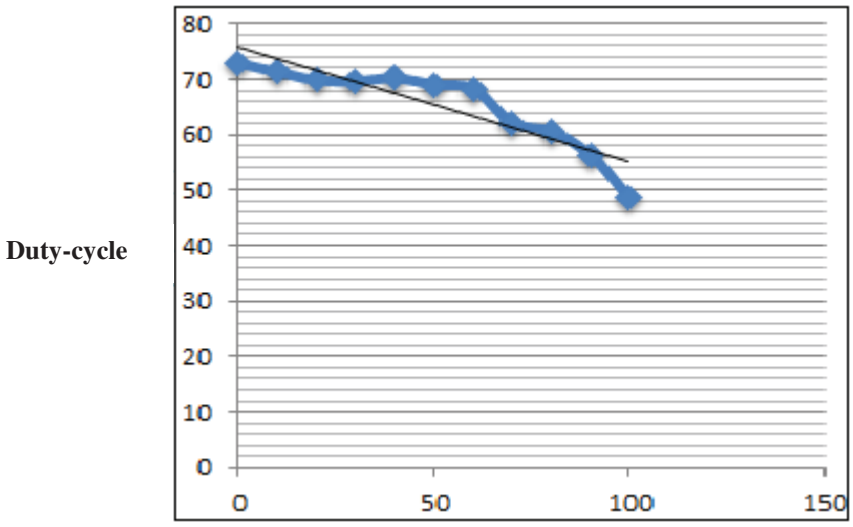

Figure 5.29 Graphical representation of output duty cycle with change in R_t (Ω)

- **The graph drawn between change in resistance to the original resistance and dc voltage.**

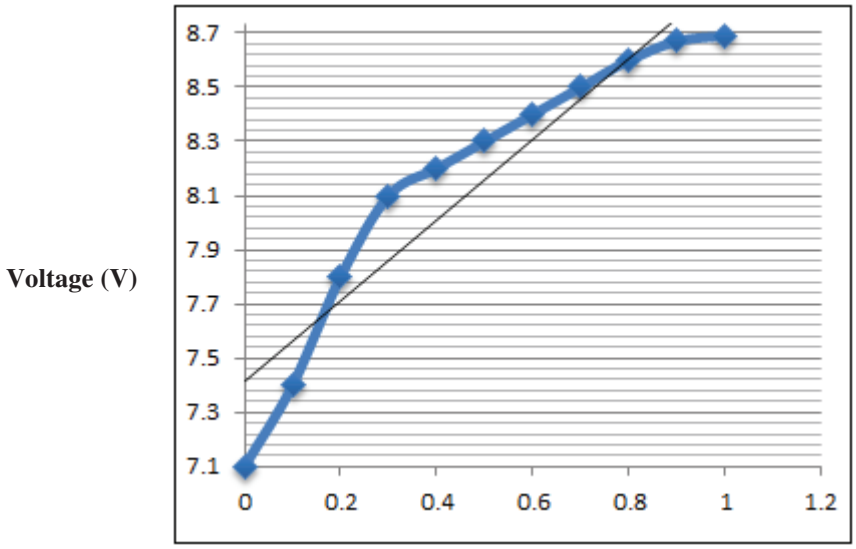

Figure 5.30 Graphical representation of dc voltage with ΔR/R

CHAPTER 6

CONCLUSION AND FUTURE SCOPE

6.1 CONCLUSION

The simulated interfacing circuit for resistive sensors which will measure the change in resistance due to the moisture in the available filler material and change in temperature due to thermal stress on the cable react electrically in the form of frequency and duty-cycle respectively. It also relates with operating voltage of this interfacing circuit. Moreover, the duty-cycle is easily converted into DC analog signal using low pass filter. The high noise is delivered in remote areas of transmission and allows the digital conversion at minimum cabling and system cost.

6.2 FUTURE SCOPE

In the future time, this work is useful for following purposes:

1) From this circuit, we can get an accurate data analysis for measuring moisture content and temperature rise in the underground cables.
2) This information of moisture content and temperature with respect to the change in resistance of the sensor due to moisture in the sand and change in resistance of the another sensor due to thermal stress placed in the concrete lined trenches of high-voltage underground cables will be displayed on SCADA system in the real-time process.

REFERENCES

[1] G. J. Anders, A. K. T. Napieralski, and W. Zamojski, "Calculation of the internal thermal resistance and ampacity of 3-core unscreened cables with fillers," *IEEE Transactions on Power Delivery*, vol. 13, no. 3, pp. 699-705, July 1998.

[2] Martin G. Stewart, Wah Hoon Siew, Member, IEEE, Leslie C. Campbell, Member, IEEE, and Clive Ferguson, "Sensors System For Monitoring Soil Moisture Content in cable Trenches of High-Voltage Cables," *IEEE Trans. On power delivery*, vol. 19, no. 2, pp. 451-455, April 2004.

[3] Keith Malmedal, Carson Bates, David Cain, "The measurement of soil thermal stability, thermal resistivity, and underground cable ampacity," *IEEE Journal*, pp. 1-12, 2014.

[4] L. E. Imlay, "Effect of Moisture in the Earth on Temperature of Underground Cables*," A. I. E. E Trans. At 3d Midwinter Convention of the American Institute of Electrical Engineers*, New York, pp. 263-270, February 1915.

[5] Tarikul Islam, Lokesh Kumar, Zaheer Uddin and Amit Ganguly, "Relaxation Oscillator-Based Active Bridge Circuit for Linearly Converting Resistance to Frequency of Resistive Sensor," *IEEE Sensors Journal*, vol. 13, no. 5, May 2013.

[6] Steve Taranovich, "Humidity sensors and signal conditioning choices," *Contributed by electronic products*, October 2011.

[7] Hamid Farahani, Rahman Wagiran, and Mohd Nizar Hamidon, "Humidity sensor principle, mechanisim, and fabrication technologies: A comprehensive review," *Sensors 2014*, pp. 7881-7939, April 2014.

[8] Soni M. L., Gupta P. V., Bhatnagar U. S., and Chakrabarti A., "Power System Engineering," pp. 326-336, 2003.

[9] Eugene D. Eby, "Oil-filled terminals for high voltage cables," *A. I. E. E. Journal*, pp. 593-600, June 1925.

[10] A. N. Arman, M. Cherry, L. Gosland, and P. M. Hollingsworth, "Influence of soil-moisture migration on power rating of cables in h.v. transmission systems," *PROC. IEE,* vol. 111, no. 5, pp. 1000-1016, May 1964.

[11] Starr A. T., Generation, Transmission and Utilization of Electrical Power, *SIR ISSAC PITMAN & SONS publishers Ltd.*, 1937.

[12] Earle C. Bascom, Victor D. Antoniello, "Underground Power Cable Considerations: Alternatives to Overhead," *Presented at 47th Minnesota Power Systems Conference (MIPSYCON),* November 2011.

[13] O. R. Schurig, H. P. Kuehni, and F. H. Buller, "Losses in armoured single-conductor lead-covered A.C. cables," *A. I. E. E. Transactions*, pp. 417-434, April 1929.

[14] W. Cramp, Nora I. Calderwood, "The use of single–core sheathed cables for alternating currents," *IEEE Journal*, loc. Cil., vol no. 61, January 1923.

[15] G. B. Shanklin, "The effects of moisture on the thermal conductivity of soil," *Presented at the 10th Midwinter Convention of the A. I. E. E.*, New York, N. Y., pp. 94-102, February 1922.

[16] C. L. Wahwa, "Electrical power systems, *New age international publishers*, fourth edition, pp. 211-213, 2005.

[17] J. R. Lucas, "High-voltage engineering, pp. 65-66, 2001.

[18] Ashok Kr. Naskar, Nirmal Kr. Bhattacharya, Sourav Saha, S. N. Kundu, "Thermal analysis of underground power cables using two dimensional finite element method," *IEEE Ist International Conference on Condition Assessment Techniques in Electrical Systems*, pp. 94-99, 2013.

[19] M. A. El-Kady, F. Y. Chu, H. S. Radkrishna, D. J. Horrcks and R. W. D. Ganton, "A probabilistic approach to power cable thermal analysis and ampacity evaluation," *IEEE Transactions on Power Apparatus and Systems*, Vol. PAS-103, pp. 2735=2740, 1984.

[20] J. H. Neher and M. H. McGrath, “The calculation of temperature rise and load capability of cable systems,” *AIEE Transactions (Power Appartus and Systems)*, Vol. 76, pp. 752-772, 1957.

[21] E. J. Brooks, C. H. Gosling, and W. Holdup, “Moisture control of cable environment with particular reference to surface troughs,” *PROC. IEE*, Vol. 120, No. 1, pp. 563-566, January 1973.

[22] Vittorio Ferrari, Carla Ghidni, Daniele Mariolo, and Andrea Taroni, “Oscillator-based signal conditioning with improved linearity for resistive sensors,” *IEEE Transactions on instrumentation and measurement*,” vol. 47, no. 1, pp. 293-298, February 1998.

[23] Johan H. Huijsing, Gerard A. Van Rossum, and Matthijs Van Der Lee, “Two-wire bridge-to-frequency converter,” *IEEE Journal of solid-state circuits*, vol. sc-22, no. 3, pp. 343-349, June 1987.

[24] Won Sup Chung and Kenzo Watanabe, “A linear temperature-to-frequency converter using an integrable colpitts oscillator,” *IEEE Transactions on instrumentation and measurement*, vol. IM-34, no. 4, pp. 534-537, December 1985.

[25] Paolo Mantenuto, Andrea De Marcellis, and Giuseppe Ferri, “Uncalibrated Analog bridge-based interface for wide-range resistive sensor estimation,” *IEEE Sensors Journal*, vol. 12, no. 5, pp. 1413-1414, May 2012.

[26] Curtis D. Johnson, Hassan Al Richeh, “Highly accurate resistance deviation to frequency converter with programmable sensitivity and resolution,” *IEEE Transactions on instrumentation and measurement*, vol. IM-35, no. 2, pp. 178-181, June 1986.

[27] Ossama E. Gouda, Adel Z. El Dein, and Ghada M. Amer, “Effect of the formation of the dry zone around underground power cables on their ratings,” *IEEE Transactions on power delivery*, vol. 26, no. 2, pp. 972-978, April 2011.

[28] Ammar Anwar Khan, Nazar Malik, Abdulrehman Al-Arainy, Saad Alghuwainem, “A review of condition monitoring of underground power cables,” *IEEE International conference on Condition Monitoring and Diagnosis*, vol. A-23, pp. 909-912, September 2012.

[29] J. S. Lyall, G. Nourbaksh, H. C. Zhao, “Underground Power Cable Environment On-Line Monitoring & Analysis,” *IEEE Journal*, pp. 457-462, 2000.

[30] Chang-Young Lee, Seok-Hyun Nam, Su-Gil Lee, Dong-Wook Kim, and Myung-Kyu Choi, “High frequency partial discharge measurement by capacitive sensor for underground power cable system,” *IEEE Journal*, pp.1517-1520, 2000.